International Journal of Quantum Technologies
ISSN: 3068-9090

PRIME OPEN ACCESS

Volume 2, Issue 1

Research Article

Date of Submission: 21 Dec, 2025
Date of Acceptance: 29 Jan, 2026
Date of Publication: 20 Feb, 2026

Energetic Bilan of a Mems Conform to Emmy Noether Theorem for Extraction of Electrical Peak Power of Vacuum Energy

Dr. SANGOUARD Patrick*

Retired from Ecole Supérieure Ingénieurs Electronique Electro technique Paris France

***Corresponding Author:**
Dr. SANGOUARD Patrick, Retired from Ecole Supérieure Ingénieurs Electronique Electro technique Paris France.
sangouard2.patrick@gmail.com
+33686507844

Citation: Patrick, S. (2025). Energetic Bilan of a Mems Conform to Emmy Noether Theorem for Extraction of Electrical Peak Power of Vacuum Energy. *Int J Quantum Technol, 2*(1), 01-26.

Abstract
This theoretical work addresses the hope of extracting an energy present throughout the universe: that of the quantum vacuum. This article demonstrates that by harnessing quantum vacuum energy, it is theoretically possible to maintain a continuous periodic vibration of a piezoelectric bridge and extract usable electrical power from it, without contradicting Emmy Noether's theorem. The sensor vibrations in the proposed MEMS differ from an impossible perpetual motion, as they are permanently powered by quantum vacuum energy. They are achieved by automatically controlling the deformation of a piezoelectric bridge. This cyclical deformation is created thanks to the omnipresent, permanent, and attractive Casimir force (CAF) between two electrodes. This CAF starts at a position z0 and is controlled by an automatic Coulomb repulsion force (COF), applied by closing switch #1 on a third electrode called the Coulomb. The Coulomb force (COF) derives from the electrical charges generated by the deformation of the piezoelectric bridge. The FCO force is in the opposite direction and of greater intensity than the FCA force. It is generated at a position z1 < zo and dissipated at $z2$, with z1 < ≈ $z2$ < $z0$, by the consecutive but very close activation of two switches, which operate automatically thanks to the electrical charges produced on the deformed piezoelectric bridge. The resulting FCO - FCA force straightens the bridge and transmits kinetic energy to it and to the moving Casimir electrode. As the deformation of the piezoelectric bridge decreases, so does the voltage on the gates of switches #1 and #2, switch #1 opens again, immediately after closing. Very quickly, switch #2 switches to ground via an RLC circuit, the Coulomb electrode is then brought back to ground and the FCO force therefore disappears very quickly after its appearance. The kinetic energy acquired by the structure is then dissipated by the action of the FCA force, but confers inertia that allows the structures to return to or slightly exceed their initial position. The Casimir force, still present, then deforms the structure again. The system vibrates at a frequency and amplitude depending on its physical and geometric characteristics. Each time switch #2 is grounded, a current and voltage spike is generated. These periodic power spikes power a self-contained electronic circuit (without power supply) that transforms these signals into a usable DC voltage. In this article, we will primarily present the structure's energy balance and demonstrate its consistency with Emmy Noether's fundamental theorem.

Keywords: Casimir, Coulomb, Vacuum Quantum Energy Extraction, Piezoelectric, MEMS

Description of the system
Introduction
We know that the quantum vacuum, the energy vacuum, the absolutely nothing, does not exist.
This statement has been proven multiple times and noted by:
• Lamb's shift (1947) of atomic emission frequencies:
https://quantummechanics.ucsd.edu/ph130a/130_notes/node476.html)
• By the force of Van der Waals which plays a very important physicochemical role and had an interpretation quantum 1930 [London] when two atoms are coupled to the same fluctuations in vacuum:

https://culturesciences.chimie.ens.fr/thematiques/chimie-du-vivant/les-forces-de-van-der-waals-et-le-gecko
• By Hawking's radiation theory, predicted in 1974 and observed on September 7, 2016. Article Observation of quantum Hawking radiation and its entanglement in an analogue black hole : https://www.nature.com/articles/nphys3863
• By the experimental verification (1958) of the existence of a force equated by Casimir in 1948. This so-called Casimir force was measured for the first time in 1997: https://arxiv.org/abs/quant-ph/9907076 https://en.wikipedia.org/wiki/Casimir_effect

The undisputed interpretation of the above effects involves an energy source coming from some kind of "nothing" or more precisely from the quantum vacuum. So, it is certain that this source of energy causing unmistakable physical manifestations exists. We will therefore choose, for the remainder of this article, a reference frame consisting of the 4-dimensional "Space-time" continuum augmented by those, still unknown, in the "quantum vacuum". In this reference frame we will try to show that the mathematical theorem of the mathematician Emmy Noether is not transgressed. This important mathematical theorem involves in other things the conservation of energy: https://fr.wikiversity.org/wiki/Outils_math%C3%A9matiques_pour_la_physique_(PCSI)/Th%C3%A9or%C3%A8me_d%2 7Emmy_N%C5%93ther#
In this paper we will focus essentially on presenting the detailed energy balance of a MEMS apparently capable of permanently extracting a small amount of energy from the quantum vacuum that can be used in our world. We will try to show that using a piezoelectric bridge deformed by a isotropic , atemporal , attractive, force of Casimir FCA , and straightened by a very ephemeral , repulsive , but more intense force of Coulomb FCO induced by this deformation , an apparent "perpetual movement" of the MEMS device is possible .The schematic of this M.E.M.S. is in figure 4 and 5

In fact, the problem is less to extract energy from the vacuum than to extract it without spending more energy that we $\pi 2\ c\ \mathrm{h}$ cannot hope to recover. The attractive Casimir force is $F_{CA} = S_S \frac{\pi^2\ c\ \hbar}{240\ z_S{}^4}$ (Eq.1),ref .With SS the surface of [1-3].

With S_S the surface of Casimir's electrodes , $\hbar = \mathrm{h}/2\pi$ the reduce Planck constant, and c the speed of light, z_s the interface of Casimir's electrodes . This variation in $1/z_s^4$ of FCA , would imply that a larger opposing force is provided to return to the initial position when the interface z_s is smaller.

Coulomb's force can play this role with an energy balance satisfying Emmy Noether's theorem, because -as we shall see- this force will be in $1/z_s^{10}$: In fact, we know that the fixed charges QF induced by a Casimir force F_{CA} - in the case of a deformation perpendicular to the polarization of a piezoelectric film- are proportional to the Casimir force FCA and are therefore in $1/z_s^4$. We have, with z_0 the initial position without any deformation of the piezoelectric film:

$\mathrm{Q_F} = \frac{d_{31}\ l_p}{a_p}\ F_{CA} \Rightarrow \mathrm{Q_F} = \frac{d_{31}\ l_p}{a_p}\ \mathrm{S}\ \frac{\pi^2\ \mathrm{c}\ \hbar}{240}\left(\frac{1}{z_S^4} - \frac{1}{z_0^4}\right)$ (Eq. (2)),ref [4-6]. In this expression when $z_s = z_0$ the electric charge is null . The piezoelectric coefficient is d_{31} (CN^{-1}), l_p, a_p , are respectively length and thickness (m) of the piezoelectric bridge. Q_F does not depend on the common width bp = bs = bi of the structures (figure 4,5,6). This point is interesting and facilitates the technological realization of these structures since it limits the difficulties of their deep and straight engraving. These fixed electric and ionic charges Q_F , inside the piezoelectric bridge, have opposite signs and induce an electric field that attract from the mass and on the two metallized faces of this bridge , mobile charges of opposite signs.

The mobile charges, for example on face 2 (Figure 4,5), of the faces of the bridge activate the insulating gates of the enriched transistors Thin Film Transistor Metal Oxide Semiconductor T.F.T. M.O.S , N and P in parallel of switch n°1 (Fig 2)[11]. It generates on these transistors a gate voltage V_G with the expression $V_g = \frac{Q_F}{C_{ox}}$ (Eq.3) . With, Cox the capacity of the grid's transistors $C_{ox} = \frac{\varepsilon_{\cdot 0}\varepsilon_{ox}}{t_{ox}}\ L_T W_T$ (Eq.4) and ε_o the permittivity of vacuum, ε_{ox} the relative permittivity of silicon oxide , L_T , W_T ,t_{ox} the length, width and thickness of the grid of the TFT MOS . The mobile charges of the other face 1 (Fig 4,5) of the bridge supply the sources of the T.F.T. M.O.S. N and P and can circulate to homogenize on a so-called Coulomb electrode, if the threshold voltage of the switch n°1 is exceeded. Before closing switch n°1, this Coulomb electrode was grounded by closing switch n°2, consisting of N and P M.O.S. T.F.T 's in depletion and in series.(Fig 3). It is important to note that:
1/ The threshold voltage values of these switches are V_{T1} for switch n°1 and VT2 for switch n°2, and that $|V_{T1}|$ very slightly above $|V_{T2}|$ with some tens of millivolts 2/ If the voltage on the insulating gates of the MOS TFTs is above their threshold voltage then: Switch n°1, changes from OFF to ON but conversely switch n°2 changes from ON to OFF (Figure 1)

Description of Switches n°1 or n°2 and Autonomous Electronic Switches Electronic Description

These indispensable switches are made with:
a/ Circuit n°1 (figure 2): with T.F.T. MOS P and MOS N transistors enriched and in parallel: Threshold voltage VTNE and VTPE b/ Circuit n° 2 (figure 3): with T.F.T. MOS P and MOS N transistors in depletion and in series: Threshold voltage VTND and VTPD

An important point is that the threshold voltage values of these transistors are positioned as Figure 1.

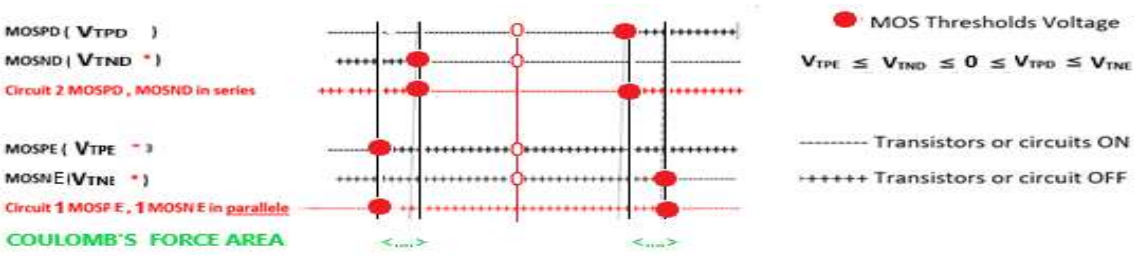

Figure 1: Distribution of the Threshold Voltages of Enriched and Depleted N and P MOS Switches.

We have : $V_{TPE} < V_{TND} < 0 < V_{TPD} < V_{TNE}$. For the functioning symmetry $|V_{TPE}|$ can equal $|V_{TNE}|$ and $|V_{TPD}|$ can equal $|V_{TND}|$. Consequently, as $|V_{TND}| < |V_{TPE}|$ and $|V_{TPD}| < |V_{TNE}|$, and with a difference of their values of just some tens of millivolts , circuit switch n° 2 commute , then is open or closed *just before* circuit switch n° 1 switches respectively from closed or open (see figure n° 1, 2,3, 4, 5 , 6, 18).

Circuit n°1: Switch n° 1

Switch n°1 consists -with their threshold VTNE or VTPE voltage- of enriched N type TFT MOS , in parallel with an enriched P type TFT MOS (fig 1,2), as positioned in fig 2. [11]

(Figure 2)
Switch n°1

The common gates voltage of these enriched T.F.T. MOS N and P in parallel of switch n°1(figure 2), are controlled by the free charges appearing on face n°2 of the piezoelectric bridge. The N and P sources of these T.F.T. MOS are connected to face n° 1 of the bridge and the drains Coulomb's electrode. (Figure 4,5).

The switch n°1 is make with two types of enriched MOSPE or MOSNE transistors in parallel, to avoid the exact nature (holes or electrons) of the mobile electric charges appearing on the metal face n°1 of the piezoelectric bridge. Preferably, their threshold voltages are the same in absolute value $|V_{TNE}| = |V_{TPE}|$. The input of the R.L.C circuit is connected in series between the return Coulomb electrode and the ground, the autonomous electronic n°3 in parallel (figure 4,5). This return Coulomb electrode is itself grounded via switch n°2

Circuit 2: Switches n°2

Switch n°2, consists of a P type depletion T.F.T. MOSPD in series with an N type MOSND depletion (see figure 1,3 ,5). The common gates of these MOS switches are controlled by the free charges appearing on face n°2 of the piezoelectric bridge. (figure 1,4,5). The input of switch n°2 is connected to the Coulomb electrode, and its output to the RLC circuit, then to ground. Preferably, their threshold voltages are the same in absolute value $|V_{TND}| = |V_{TPD}|$. The values of $|V_{TND}| \approx |V_{TPD}|$ are lower but very close (down than 10 %) of $|V_{TNE}| \approx |V_{TPE}|$

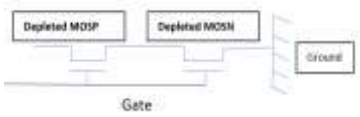

(Figure 3)
Switch n°2

schematic and comportment of the MEMS

Thus, when it is effective (switch n°1 closed), the Coulomb return force FCO is (Figure 4,5,6)

$$F_{CO} = \frac{Q_F^2}{4\,\pi\,\varepsilon_0\,\varepsilon_r}\left(\frac{1}{z_r + z_0 - z_s}\right)^2 = \left[\frac{d_{31}\,l_p}{a_p}\,S_S\,\frac{\pi^2\,c\,\hbar}{240}\left(\frac{1}{z_s^4} - \frac{1}{z_0^4}\right)\right]^2\left(\frac{1}{8\,\pi\,\varepsilon_0\,\varepsilon_r}\right)\left(\frac{1}{z_r + z_0 - z_s}\right)^2 \quad \text{(Eq. 5)}$$

We note that FCO is in $1/z_s^{10}$, with z_s = distance (time dependent) between Casimir electrodes, and z_0 = initial distance between Casimir electrodes (without any electric's charges) . The schematic of the sensor part of this MEMS is shown in figures (4 ,5). The perpetual, isotropic and timeless Casimir F_{CA} force, resulting from quantum vacuum fluctuations, causes the deformation of a microscopic piezoelectric bridge embedded in a silicon wafer.

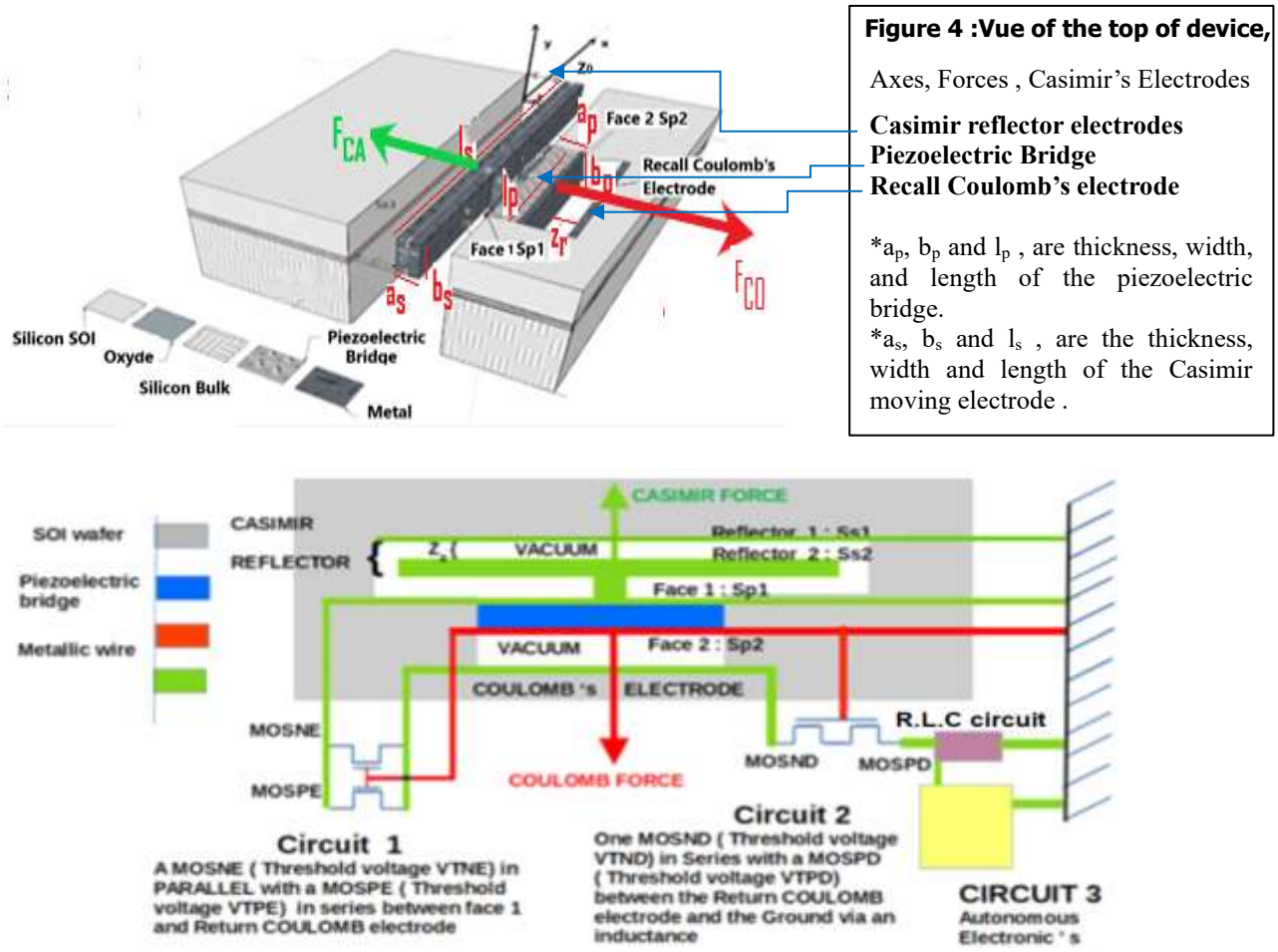

Figure 5: general configuration of the device: MOS grid connections (Face 2 of the piezoelectric bridge: red), Source connections (Face 1 of the piezoelectric bridge: green)

We remark that the Casimir force FCA appearing between the reflector electrodes (green) is applied to the piezoelectric bridge (blue) via a metallic digit (green) When the switch n°1 is open, the mobiles charges of face n°1 don't move and keep on this face n°1. When the switch n°1 is closed and switch n°2 is open, the free moving electric charges must homogenize between the metallic film of face n°1 and the metallic film of Coulombs electrode (Figure 4,5). If the area of Face 1 of the piezoelectric bridge and the area of the electrode Coulomb are equal, then the charge on this electrode is $Q_F/2$. Then, as the electrical nature of mobiles charges of faces n°1 and n°2 are opposite, Coulomb's force FCO must appear between these two metallic electrodes. The threshold voltages of the transistors of switch n°1, technologically predetermined, impose the intensity of Coulomb's forces, which can be much greater than the force of Casimir FCA. The Coulomb force's lifespan is ephemeral, and its dissipated energy is determined by the threshold voltages of switch n°2, when it is closed to ground (Figure 1,3,4,5,6). The resulting force FCO - FCA, applied to the center of the piezoelectric bridge, changes direction or is zero. The piezoelectric and elastic bridge having no force to keep it deformed, necessarily returns (by the stored deformation energy + the kinetic energy) to its initial position, therefore without any deformation or electrical charges. This ephemeral Coulomb force suppresses the collapse of the two very close electrodes of the Casimir reflector and reduces, then cancels the deformation of the piezoelectric bridge, and thus its electric charges. The structure returns to its initial state and is again deformed by the timeless and isotope Casimir force FCA, which always exists. (Figure 6)

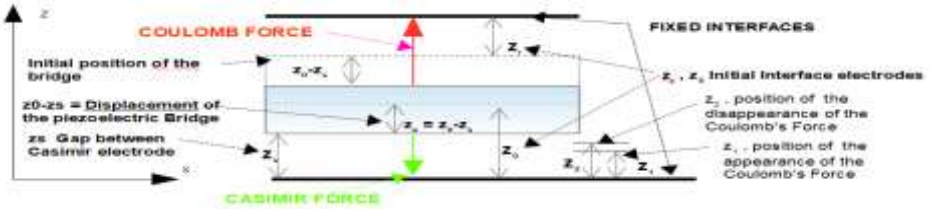

Figure 6: Axes, Forces , Casimir's Electrodes

This cycle reproduces itself and the system vibrates (Figure 8,9,10) , with the vacuum energy transmitted by the FCA force, as a continuous drive source for the deformation of the piezoelectric bridge and with the self-built Coulomb force FCO, superior and opposed to FCA as the counter-reaction force. At each cycle, the automatic switching of the integrated switches of circuits n°1 and n°2 (Figure 1,2,3,4,5,6) distributes differently the mobile electrical charges located on face n°1 of the bridge.

Notice that initially, the Coulomb's electrode was grounded by the automatically closing of the switch n°2 (Figure 1,3)

Calculation of the behaviour of the structure

Let us calculate the evolution in time of the deflection of the piezoelectric bridge due to the Casimir's force which is applied between the two electrodes separated by an initial distance z_0 (Figure 5). We use the theorem of angular momentum for this vibrating structure.(Eq. 6)

$$\overrightarrow{\sigma^{S}_{Ax,y,z}(\ Structure)} = \overline{I^{S}_{A\,x,y,z}}\ \overrightarrow{\theta^{S}_{A\,x,y,z}} \quad \text{(Eq. 6)}$$

With $\overrightarrow{\sigma^{S}_{Axyz}}$ the angular momentum vector of the structure, I^{S}_{Axyz} the inertia matrix of the total structure with respect to the reference (A, x,y,z) and θ^{S}_{Axyz} the rotation vector of the piezoelectric bridge with respect to the axis Ay with α the low angle of rotation along the y axis of the piezoelectric bridge

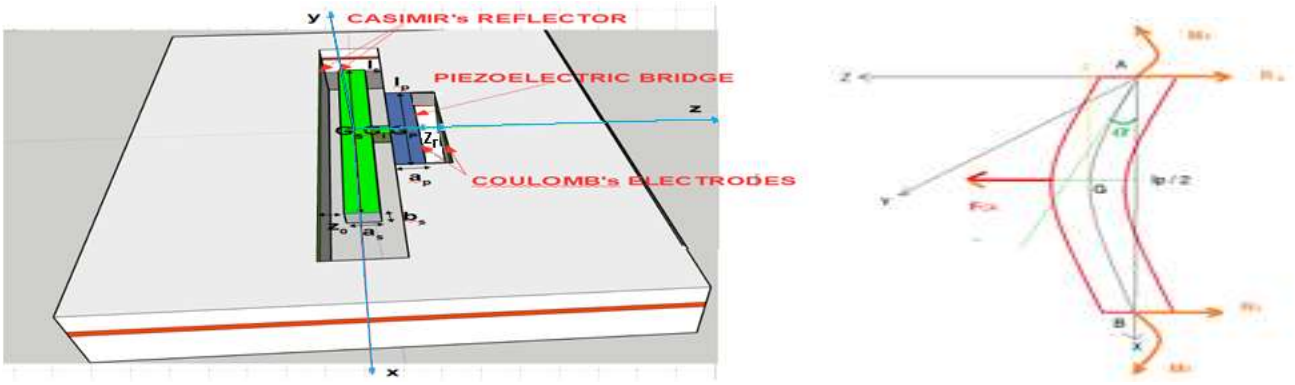

Figure 7: Piezoelectric bridge Cutting Reactions and Bending Moment, Deflection

We have $\overrightarrow{\theta^{S}_{A}} = \begin{pmatrix} 0 \\ d\alpha/dt \\ 0 \end{pmatrix}$ with $d\alpha/dt \approx \frac{2}{l_p}\frac{dz}{dt}$ because $\sin(\alpha) = \sin\left(\frac{2z_s}{l_p}\right) \approx \frac{2z_s}{l_p}$ as $z << l_p$

Let (Gp, x, y, z), (Gi, x, y, z), (Gs, x, y, z) be the barycentric points respectively of the piezoelectric bridge, of the connecting metal finger and of the metal block constituting the mobile sole of the Casimir reflector. We have (fig 4,5):

$$\overrightarrow{AG_{p,x,y,z}} = \frac{1}{2}\begin{pmatrix} l_p \\ b_p \\ a_p \end{pmatrix} \quad \overrightarrow{AG_{i,x,y,z}} = \frac{1}{2}\begin{pmatrix} l_p + l_i \\ b_p + b_i \\ a_p + a_i \end{pmatrix} \quad \overrightarrow{AG_{s,x,y,z}} = \frac{1}{2}\begin{pmatrix} l_p + l_i + l_s \\ b_p + b_i + b_s \\ a_p + a_i + a_s \end{pmatrix}$$

The inertia matrix of the bridge, in the frame of reference (Gp, x, y, z) is:

$$I^{P}_{GP} = \frac{m_p}{12}\begin{pmatrix} a^2{}_p + b^2{}_p & 0 & 0 \\ 0 & l^2{}_p + b^2{}_p & 0 \\ 0 & 0 & a^2{}_p + l^2{}_p \end{pmatrix}$$

Taking Huygens' theorem into account, this inertia matrix becomes

$$I^{P}_{A,x,y,z} = m_p\begin{pmatrix} \frac{a^2{}_p + b^2{}_p}{3} & -\frac{l_p b_p}{4} & -\frac{l_p a_p}{4} \\ -\frac{l_p b_p}{4} & \frac{a^2{}_p + l^2{}_p}{3} & -\frac{a_p b_p}{4} \\ -\frac{l_p b a}{4} & -\frac{a_p b_p}{4} & \frac{l^2{}_p + b^2{}_p}{3} \end{pmatrix} \text{(Eq (7)):}$$

With the same reasoning we can calculate the inertia matrix of the finger $I^{I}_{A,\,x,\,y,\,z,}$ and the inertia matrix of the reflector $I^{c}_{A,\,x,\,y,\,z}$ in the frame of reference (A, x, y, z),

$$I^{I}_{A,x,y,z} = \frac{m_i}{12}\begin{pmatrix} a_i^2 + b_i^2 & 0 & 0 \\ 0 & a_i^2 + l_i^2 & 0 \\ 0 & 0 & l_i^2 + b_i^2 \end{pmatrix} + m_i \begin{pmatrix} \frac{(b_p+b_i)^2+(a_p+a_i)^2}{4} & -\frac{(b_p+b_i)(l_p+l_i)}{4} & -\frac{(a_p+a_i)(l_p+l_i)}{4} \\ -\frac{(b_p+b_i)(l_p+l_i)}{4} & \frac{(l_p+l_i)^2+(a_p+a_i)^2}{4} & -\frac{(b_p+b_i)(a_p+a_i)}{4} \\ -\frac{(a_p+a_i)(l_p+l_i)}{4} & -\frac{(b_p+b_i)(a_p+a_i)}{4} & \frac{(b_p+b_i)^2+(l_p+l_i)^2}{4} \end{pmatrix} \text{(Eq. (8))}$$

$$I^{C}_{A,x,y,z} = \frac{m_s}{12}\begin{pmatrix} a_s^2 + b_s^2 & 0 & 0 \\ 0 & a_s^2 + l_s^2 & 0 \\ 0 & 0 & l_s^2 + b_s^2 \end{pmatrix} + m_s \begin{pmatrix} \frac{(b_p+b_i+b_s)^2+(a_p+a_i+a_s)^2}{4} & -\frac{(l_p+l_i+l_s)(b_p+b_i+b_s)}{4} & -\frac{(l_p+l_i+l_s)(a_p+a_i+as)}{4} \\ -\frac{(l_p+l_i+l_s)(b_p+b_i+b_s)}{4} & \frac{(l_p+l_i+l_s)^2+(a_p+a_i+a_s)^2}{4} & -\frac{(b_p+b_i+b_s)(a_p+a_i+as)}{4} \\ -\frac{(l_p+l_i+l_s)(a_p+a_i+as)}{4} & -\frac{(b_p+b_i+b_s)(a_p+a_i+as)}{4} & \frac{(b_p+b_i+b_s)^2+(l_p+l_i+l_s)^2}{4} \end{pmatrix} \text{(Eq. (9)}$$

The total inertia of the structure becomes in the reference (A, x, y, z) is : $I^{s}_{A,x,y\,z} = I^{P}_{A,x,\,y,\,z} + I^{I}_{A,\,x,\,y,\,z} + I^{c}_{A,\,x,\,y,\,z}$ with A at the edge of the recessed piezoelectric bridge .The angular momentum theorem applied to the whole structure gives :

$$\frac{\overrightarrow{d(\sigma^{S}_{A,x,y,z})}}{dt} \overline{-I^{S}_{A,x,y,z}} \frac{\overrightarrow{d\theta^{x}_{A}}}{dt} \rightarrow \overline{I^{S}_{A,x,y,z}} \frac{2}{I_P}\begin{pmatrix} 0 \\ \frac{d^2z}{dt^2} \\ 0 \end{pmatrix} - \sum_{A} \overrightarrow{Moments\ of\ the\ structure} - \text{Eq. (10)}$$

$$-\overrightarrow{M_A} + \overrightarrow{M_B} + \overrightarrow{F_{CA}} \wedge \begin{pmatrix} l_P/2 \\ 0 \\ 0 \end{pmatrix} with\ \overrightarrow{F_{CA}} - \begin{pmatrix} 0 \\ 0 \\ F_{CA} \end{pmatrix}$$

The structure rotates around the Ay axis, the moments at point A are $M_{AY} = M_{BY} = - F_{CA}$ lp /8 [10], therefore the summation of Moments on the structure relative to the axe Ay = 1/4*lp * F_{CA} . Any calculation done; we obtain:

$$\overline{I^{s}_{y}} \frac{2}{I_P} \frac{d^2z}{dt^2} = \frac{I_P}{4} F_{CA} = \frac{I_P}{4} S_S \frac{\pi^2 \hbar c}{240\ z^4}$$ with I^{S}_{y} the inertia of the structure relatively to the axe Ay.

$$I^{S}_{Y} = \rho_P a_P b_P l_P \left(\frac{\left(l_P^2 + a_P^2\right)}{12} + \frac{\left(l_P^2 + a_P^2\right)}{4}\right) + \rho_i a_i b_i l_i \left(\frac{\left(l_i^2 + a_i^2\right)}{12} + \frac{\left(l_p + l_i\right)^2 + \left(a_P + a_i\right)^2}{4}\right) + \rho_s a_i b_i l_i \left(\frac{\left(l_i^2 + a_i^2\right)}{12} + \frac{\left(l_p + l_i + l_s\right)^2 + \left(a_P + a_i + a_s\right)^2}{4}\right) \text{Eq.(11)}$$

With ρ_P , ρ_i , ρ_S , respectively the densities of the piezoelectric bridge , the intermediate finger and the mobile electrode of the Casimir reflector . By equation 6, we obtain the differential equation which makes it possible to calculate the interval between the two electrodes of the Casimir reflector as a function of time during the "descent" phase when the Coulomb forces are not present.

$$\frac{d^2z}{dt^2} = \frac{l_P^2}{8\ I_Y^S} S_S \frac{\pi^2 \hbar c}{240} \frac{1}{z^4} = \frac{B}{z^4}\ with\ B = \frac{l_P^2}{8\ I_Y^S} S_S \frac{\pi^2 \hbar c}{240}$$ Eq.(12). This differential equation unfortunately does not have a literal solution, and we programmed it on MATLAB to calculate the duration of this "descent" of free Casimir electrode. This duration depending on the desired value of the coefficient of proportionality p = F_{CO}/F_{CA} . (See figures chapter 4).

Just at the closing switch n°1, we have F_{CO} = p F_{CA} with p , a coefficient of proportionality defined by the threshold voltages of the MOS interrupters. Just at the end of "descent" and the start of the charge transfer , the total force F_T exerted becomes: $F_T = F_{CA} - F_{CO} = F_{CA}$ (1-p). The "descent" time of the free Casimir electrode will therefore stop when F_{CO} = - p F_{CA} . We can calculate this point z_1 where F_{CO} = p F_{CA} . We know that :

1 / The Casimir force is variable in time, but its equation is (Eq. (1)): $F_{CA} = \frac{d(E_{CA})}{dz} = S\left(\frac{\pi^2 \hbar c}{240\ z_4^4}\right)$ 2 / The mobile charges transiting from side 1 to the Coulomb electrode through circuit 1 variable also with time (Eq. (2)) are: $Q_{m} \approx \frac{Q_{m1}}{2} - \frac{d_{31}\ F_{CA}\ l_P}{2\ a_P}$ because they have the same area . 3 / The Coulomb force (Eq 5), variable over time, acting in opposition to the Casimir force :

$$F_{CO} = \left(\frac{d_{31}\ l_P}{a_P}\ l_S\ b_S\ \frac{\pi^2 \hbar c}{240}\left(\frac{1}{z_s^4} - \frac{1}{z_0^4}\right)\right)^2 \left(\frac{1}{8\ \pi\ \varepsilon_0\ \varepsilon_r}\right)\left(\frac{1}{z_r + z_0 - z_s}\right)^2 = \text{(Eq. 13)}$$

$$p\ F_{CA} = p\ l_s b_s\ \frac{\pi^2 \hbar c}{240}\ \frac{1}{z_s^4}$$

So, the "descent" of the free Casimir electrode stops when the inter electrode interface z_s is such that:

$$z_S^4\left(\left(\frac{1}{z_R+z_0-z_S}\right)^2\left(\frac{1}{z_s^4}-\frac{1}{z_0^4}\right)^2\right)-\frac{1920\ p\ \varepsilon_0\ \varepsilon_r}{\pi\hbar c\ S_S}\left(\frac{a_P}{d_{31}\ l_P}\right)^2 \text{(Eq. (14) See (Fig 18)}$$

This programmable equation gives the time td of the "descent" of the structure submitted to the Casimir force and: a/

$$F_T=(1-p)\ F_{CA}\Rightarrow(1-p)\ S_S\frac{\pi^2\hbar c}{240\ z_{sm}^4}<0\ \ if\ \ p>1$$

depend on the coefficient of proportionality p:

b/ is calculable and will stop when the inter-electrode interface z_s has a value z1 satisfying equation (14).

During all the phase where $0 < VT_{ND} < V_{GRIDS} \leq VT_{NE}$, or $VT_{PE} \leq V_{GRIDS} < VT_{ND} < 0$. The total force, variable over time and exerted at the center of the piezoelectric bridge, becomes:

$$F_T=F_{CA}-F_{CO}=S_S\frac{\pi^2\hbar c}{240\ z_S^4}-\frac{1}{2}\left[\frac{S_S\pi^2\hbar c}{240}\left(\frac{1}{z_s^4}-\frac{1}{z_0^4}\right)\left(\frac{d_{31}l_P}{a_P}\right)\right]^2\left(\frac{1}{4\pi\varepsilon_0\varepsilon_r}\right)\left(\frac{1}{z_r+z_0-z_s}\right)^2 \text{ Eq. (15) .}$$ The piezoelectric bridge subjected to this new force F_T rises towards a position where the Coulomb's F_{CO} disappears at the point z_2 (fig xx), because the switch n° 2 closed to ground, via a R.L.C. circuit (fig 4,5) . When FCO disappears, the whole moving structure (Casimir reflector electrode + finger + piezoelectric bridge) with an important masse M_t , acquires a kinetic energy E_C with $E_c=\frac{1}{2}M_tV_t^2$ and $M_t=\rho_P(a_pb_pl_p)+\rho_i(a_ib_il_i)+\rho_s(a_sb_sl_s)$, Vt= speed of the mobile structures , ρ_p , ρ_i, ρ_s , a_p b_p l_p , a_i b_i l_i , a_s b_s l_s , respectively the volumic mass and volume of the piezoelectric bridge, finger and Casimir electrode .

Let us calculate an approximation of the duration of this "rise" of the mobile electrode Casimir's reflector + finger + piezoelectric bridge , triggered when $F_{CO} = p\ F_{CA}$. This time is approximated because when the Coulomb force F_{CO} stop (because the closing of the switch n° 2 to ground at the point z_2 between z_1 and the initial point z_0 , Fig 6), the mobile structure loses its kinetic energy E_c plus its deformation energy with the braking force provided by the Casimir force. We approximate this return time by saying that point z_2 of the loss of the Coulomb force occurs at the initial point z_0. In these conditions, to know the time taken by the structure to "go back" to its neutral position, we must solve the following differential equation:

$$\frac{d^2z}{dt^2}=\frac{l_P^2}{8I_S^Y}\left(F_{CA}-F_{CO}\right)=\frac{l_P^2}{8I_S^Y}\left\{\left(l_Sb_S\frac{\pi^2\hbar c}{240\ z_S^4}\right)-\frac{1}{2}\left[l_Sb_S\frac{\pi^2\hbar c}{240}\left(\frac{d_{31}l_P}{a_P}\right)\left(\frac{1}{z_s^4}-\frac{1}{z_0^4}\right)\right]^2\right\}\left(\frac{1}{4\pi\varepsilon_0\varepsilon_r}\right)\left(\frac{1}{z_r+z_0-z_S}\right)^2 \text{Eq.(16)}$$

This differential equation (17) has no analytical solution and can only be solved numerically.

We programmed it on MATLAB. In these MATLAB simulations we considered that the metal of the electrodes and metal block was oxidized over a thickness allowing to have an interface between Casimir electrodes of 200 A ° which modifies the mass and the inertia of the vibrating structure (See chapter 5). It turns out that the choice of aluminium as the metal deposited on these electrodes is preferable given:
1 / The ratio between the thickness of the metal oxide obtained and of the metal attacked by the thermal oxidation (see chapter 6) 2 / Its low density increase and optimise the vibration frequency of the structure by minimising the inertia of the Casimir reflector and the parallelepiped block that transfers the Casimir force.

The mass $M_{structure}$ of the vibrating structure is then: $M_{STRUCTURE}= d_{pm}(a_s\ b_s\ l_s+ a_i\ b_i\ l_i) +2\ d_{om}\ z_{of}\ (a_{s0}\ b_{so}+b_{so}\ l_{so}+a_{so}\ l_{so})+d_p(a_p\ b_p\ l_p)$. With dpm the density of the metal, as, bs, ls the geometries of the final metal part of the Casimir electrode sole, dom the density of the metal oxide, a_{so} , b_{so} , l_{so} the geometries of the oxidized parts around the 6 faces of the metal block, d_p the density of the piezoelectric parallelepiped (see figure 4,5):

simulation of devices with different piezoelectric bridge

We present below the results of the MATLAB simulations carried out by numerically calculating the differential equations (11) and (13). These numerical calculations give the vibration frequency of the structure which, as we will see, vibrates at a frequency lower than its first resonant frequency (IV) . This vibration frequency depends on the characteristics of the structure (Nature of material, geometric dimensions, coefficient of proportionality $p = F_{CO} / F_{CA}$ ...)) .The metal used for the Casimir reflector block is Aluminium with a density of 2.7 g cm^{-3}.

PMN-PT piezoelectric materials for the piezoelectric bridge

To increase the density of electric charges at the terminals, piezoelectric material PMN-PT can be used. It can be deposited by RF-magnetron sputtering with a composition, for example: PMN-PT= (1-x) $\mathbf{P_b}$ (1/3 $\mathbf{M_g}$– 2/3 $\mathbf{N_b}$) O_3- x $\mathbf{P_b}$ $\mathbf{T_i}$ O_3; with piezoelectric coefficient d_{31} = 1450 .10^{-12} C / (kg .m .s^{-2}) and a Young's modulus Ep = 150 .10^9 Kg M^{-1} T^{-2}.

With MATLAB simulation, and for an interval between Casimir electrode z_0= 200 Angstroms, we obtain the evolution over time of the Casimir and Coulomb forces as well as the F_{CO} / F_{CA} ratio of figures 8 to 22 below. For a ratio p= F_{CO} / F_{CA} of 1000, the maximum current I delivered by the vibrating structure, the threshold voltage of the MOSE and the vibration frequency of the structure are respectively: I=1.2 10^{-4} A, Vt = 3.2 V and 957000 Hertz.

Evolution of the Casimir interface as a function of time during two periods: PMN-PT

The F_{CO} / F_{CA} ratio = 10000 induces a period of 3.85 10^{-6} s and a rise time of 21.3 10^{-9} s with a deflection of the bridge of 105 A °. The structure vibrates at 259.7 kHz. Due to inertia, at the rise sequence, the structure exceeds the initial 200 A ° by 20 A ° (Figure 28).

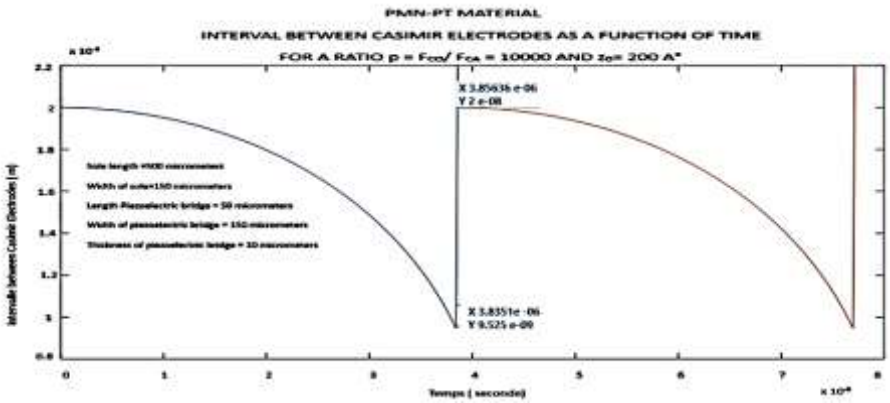

Figure 8: plot of the evolution of the Casimir inter-electrode interval as a function of time over two periods and an Fco / Fca Ratio = 10000: Casimir inter-electrode interface = 200 A°

A ratio F_{CO} / F_{CA} = 1000 induces a period of 2.96 10^{-6} s and a rise time of 44.5 10^{-9} s with a deflection of the bridge of 50 A ° The structure vibrates at 337.8 kHz: (Figure 29). For this ratio of 10000 we notice a vibration amplitude of 50A ° , a period of 2.96 10^{-6} s, with the faster rise of the mobile electrode producing a slight rebound of 5A, because of the inertia of the structure.

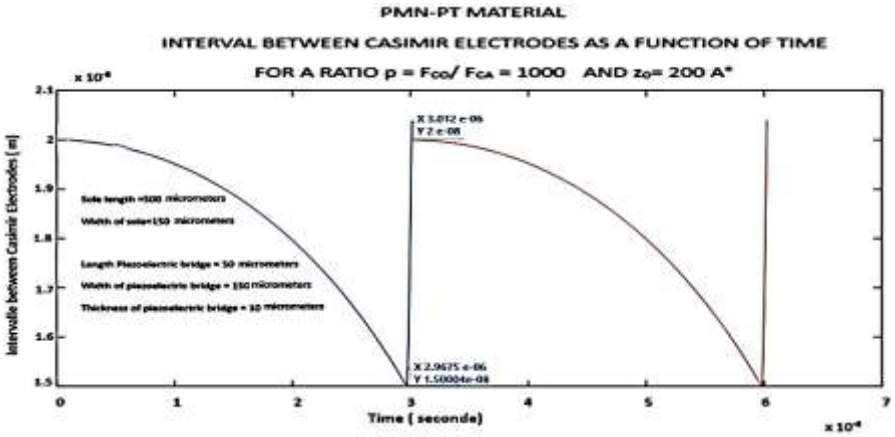

Figure 9: plot of the evolution of the Casimir inter-electrode interval as a function of time over two periods and Fco / Fca Ratio = 1000: Casimir inter-electrode interface = 200 A°

For the ratio F_{CO} / F_{CA} = 2 (Figure 30) a vibration amplitude of just 0.27 A ° and a period of 1.8610^{-7} s is obtained This low deformation of the PMN-PT piezoelectric bridge is mainly due to the extremely high piezoelectric coefficient d_{31} of 1450 (pC/N) of PMN-PT compared to 120 (pC/N) for PZT.

We observe the weak overshoot of the initial interface.

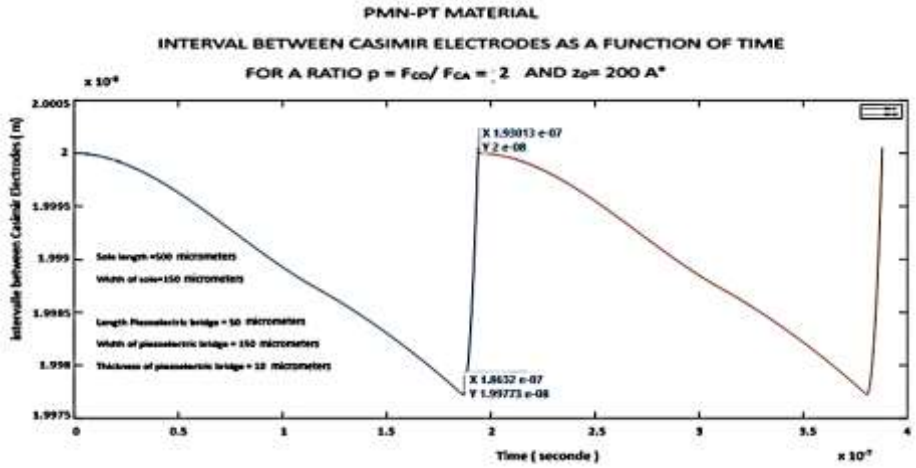

Figure 10: plot of the evolution of the Casimir inter-electrode interval as a function of time over two periods and a Ratio Fco / Fca = 2. Casimir inter-electrode interface = 200 A

Evolution of the forces of Casimir and Coulomb: PMN-PT We obtain:
1/ The evolution of the Casimir and Coulomb forces as a function
a / of the inter-electrode interface (Figure 31) and
b/ over time (Figure 32)
2/ The F_{CO} / FCA ratio as a function of time for an entire period (figures 33).

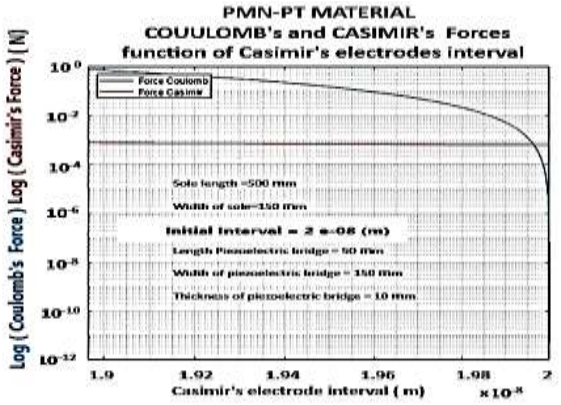

Figure 11: Materials = PMN-PT: Coulomb and Casimir force as a function of the inter-electrode interface. Start interface = 200A °

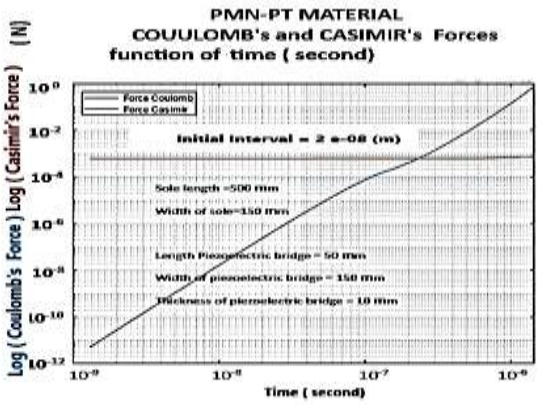

Figure 12: Materials = PMN-PT: Coulomb and Casimir force as a function of time. Start interface = 200A °

It is observed (Figure 33) that the Coulomb return force is less important for an initial inter-electrode gap zr = 400A° than for z_r= 200A°

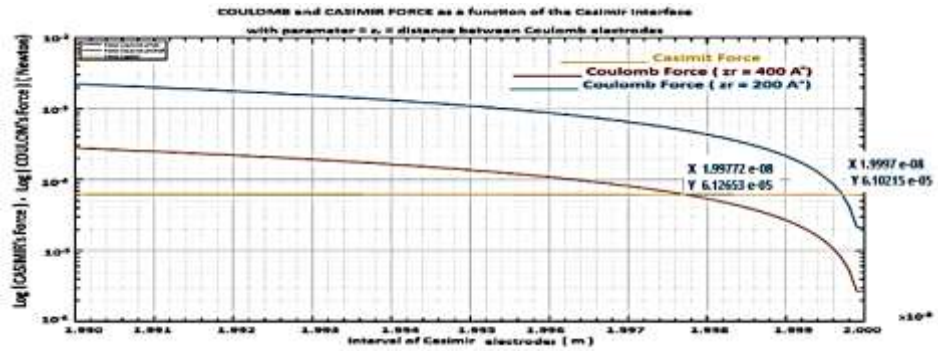

Figure 13: Materials = PMN-PT: Coulomb force for z_r = 200 A ° (Blue) and zr = 400 A ° (Red) and Casimir force (Yellow, z0 =200 A°) as a function of the inter-electrode interface Starting interface = 200 A

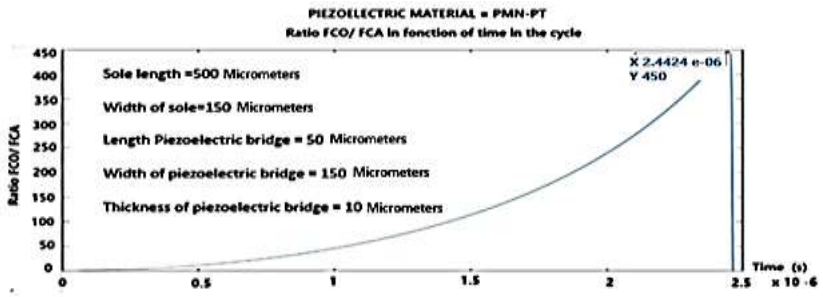

Figure 14: Materials = PMN-PT: Ratio p = FCO / FCA as a function of time, during a period of vibration. Start interface = 200A °, Maximum ratio chosen = 450

The break circuits n°1 triggered at time t = 2.44 10^{-6} s suddenly induce a rise of the mobile electrode, therefore a sudden decrease in electric charges and grids voltages. We observe the gradual evolution towards the chosen ratio of 450 and then the sudden drop in this ratio as the electrodes regain their initial position (Figure (34)).

Threshold voltage according to the desired Ratio F_{CO} / F_{CA} : PMN-PT

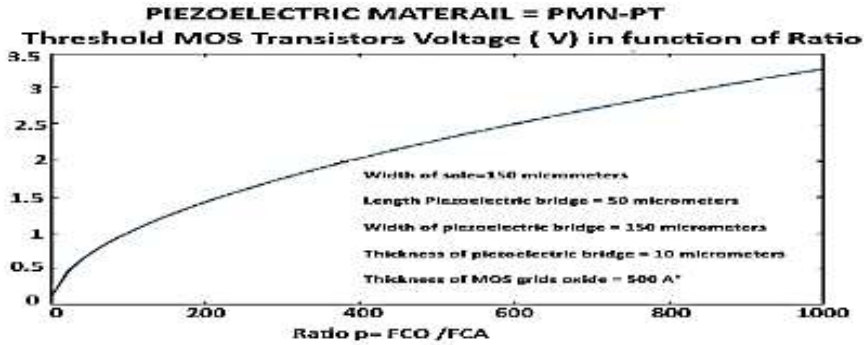

Figure 15: Materials = PMN-PT: Threshold voltage of the Enriched or Depleted MOS according to the F_{CO} / F_{CA} Ratio. Start interface = 200A °

It can be seen (Figure 15) that we must increase the threshold voltage of the TFT MOS of switch n°1 up to 3.5V if we desire to obtain a ratio FCO/FCA of 1000 .

Vibration frequency as a function of the F_{CO} / F_{CA} ratio and peak current as a function of the initial Casimir interval chosen: PMN-PT.

Note (fig 16), that for an initial interface z_0 = 200 A°, and for a ratio F_{CO} / F_{CA} = 2 , the maximum vibration frequency of the structure is 3.50 MHz . It falls to 750 kHz for a ratio of 1000. These frequencies are still lower than the first resonance of the structure, which is of the order of 7.94 Megahertz. This vibration frequency of the Casimir structure approaches that of the first resonance for weaker interfaces below 200 A°.

For a ratio F_{CO} / F_{CA} = 500, the maximum current delivered by the structure falls as a function of an increase in the initial Casimir interval (Figure 17).

It seems that the piezoelectric material PMN-PT coupled with a conductor like aluminium is an interesting couple for our vacuum energy extraction structure.

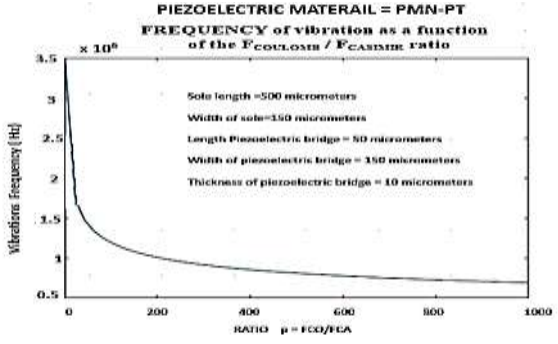

Figure 16 : Materials = PMN-PT: Vibration frequency as a function of the F_{CO} / F_{CA} Ratio. Start interface = 200A ° Start

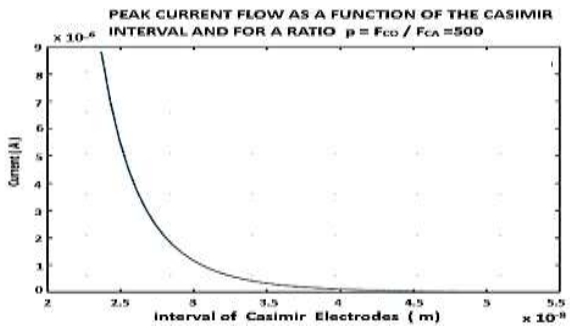

Figure 17: Materials = PMN-PT: Current peak across the 2 . 10^{-4} H inductance as a function of the starting interval between Casimir electrodes. Start interface = 200A

Mems Energy Balance

In this part, we will try to make a detailed and exhaustive assessment of the behavior of the MEMS during one vibration. Firstly, we will focus on the first half of this vibration, which we will call the "go" phase. Secondly, we will focus on the second half of the vibration, which is to say the "return" phase. Let us recall that, the piezoelectric bridge is perfectly elastic, which implies, as with any elastic structure, that the energy expended by a mechanical deformation of the positions from 0 to 1 is integrally restored when returning. The conditions of use of the piezoelectric bridge (vibrations amplitude) are in the purely elastic domain and we never enter in the domain of plasticity.

In the following we propose to put into equation the energy balance of «go» then in "return "steps .

0 < $\mathbf{VT_{PD}}$ < $\mathbf{VT_{NE}}$, and $\mathbf{VT_{PE}}$ < $\mathbf{VT_{ND}}$ **< 0 and** $\mathbf{F_{CO}}$ **/** $\mathbf{F_{CA}}$**< p** . With p the chosen amplification F_{CO} / F_{CA}. We note V_{T1}= abs (VT_{NE} or VT_{PE}) and V_{T2}= abs (VT_{ND} or VT_{PD}), and call V_G the voltage due to the mobiles charge on the face 2 of the piezoelectric bridge and appearing on the gate of all the TFT MOS transistors. [11]

MEMS energy balance during the phase "go" from z_0 to z_1

a/ 0 < $\mathbf{V_G}$ **< abs (**$\mathbf{V_{T2}}$ **)< abs(**$\mathbf{V_{T1}}$ **). and** $\mathbf{F_{CO}}$ **/** $\mathbf{F_{CA}}$**< p: switch n°1 OFF, Switch n°2 ON. (Figure 1)**

At the start, in the beginning conditions of the "go" phase, we have very small deformations applied to the piezoelectric bridge. Consequently, very small electrical charges are present on it, so the electrical voltages V_G on the grid of the enriched and parallel TFT MOS N and P of switch N°1 is lower than their threshold voltage V_{T1}. This witch n°1 is open and in the OFF position. On the other hand, as V_G < V_{T2}, switch N°2 consisting of two TFT MOS N and P in series, operating in depletion mode is closed and in the ON position to ground. In these conditions the so-called Coulomb electrode is to the ground, thus eliminating the Coulomb force F_{CO}.

b/ 0 < abs ($\mathbf{V_{T2}}$ **)<** $\mathbf{V_G}$ **< abs (**$\mathbf{V_{T1}}$**). and** $\mathbf{F_{CO}}$ **/** $\mathbf{F_{CA}}$ **< p: switch n°1 OFF, Switch n°2 OFF. (Figure 1)**

No moving electric charge appears on the return side of the Coulomb electrode, which is connected to ground by switch 2, which is ON, and isolated from the piezoelectric bridge by switch 1, which is OFF. The Casimir force begins to deform the piezoelectric bridge more significantly. Consequently, the mobiles charge on face 1 and 2 of the piezoelectric bridge therefore the voltage V_G on the gates of transistors of switch n° 1 and n° 2 increases. This voltage VG still lower than the threshold voltage V_{T1}, exceeds now V_{T2} of switch n°2 which opens and switches OFF.

The structure being assumed to be perfectly elastic and the amplitudes of the vibrations being extremely low, we will see that the mechanical energy losses by an increase of temperature in the device are negligible.

1/ Note also that the mobile parallelepiped metal electrodes of the Casimir electrodes remain parallel to each other and that the mobile metal Casimir electrode does not deform. It simply transmits its movement to the piezoelectric bridge which deforms but therefore does not heat up. (Figure 4,5)

2/ The expulsion of entropy ΔS from the vibrating structure of Casimir is transmitted to the piezoelectric bridge. It causes an extremely slight increase ΔT in its temperature and expels this heat to the outside. Let us calculate an order of this magnitude ΔT. We note ΔQ_{vib} the heat transmitted by the vibrations of the piezoelectric bridge. In first approximation, we can use the well-known formula ΔQ_{vib} = ΔS. ΔT, with ΔS= entropy variation (J °K^{-1}) and ΔT = temperature variation (°K).

However, we know that: $\Delta Q_{vib} = \frac{M_{Bridge}\,[2\,\pi\,f_{vib}]^2}{2}\,z_1^2$ Eq. (17) [10] With: f_{vib}= Vibration frequencies of the piezoelectric bridge, M_{Bridge} = mass of this bridge, which is the only one to deform because the Casimir electrodes are simply in translations. We note z_1 the maximum deflection of the bridge (Fig 6) . This heat expended at the level of the piezoelectric bridge causes its temperature to increase.

As a first approximation we can say: ΔQ_{vib} = $M_{Structure}$. C_{piezo} ΔT. With: C_{piezo} = Specific heat capacity of the piezoelectric bridge (J Kg^{-1} °K^{-1}), ΔT = Temperature variation (°K).

Consequently $\Delta T = \frac{2\,[\pi\,f_{vib}]^2}{C_{piezo}}\,z_1^2 =$ Temperature variation of the bridge. Eq. (18)

For example, for a PMN-PT piezoelectric film: C_{piezo} = $C_{PMN\text{-}PT}$ = 310 (J Kg^{-1} °K^{-1}), f_{vib} ≈ 10^6 Hz, ze100*10^{-10} m, we then obtain: ΔT 10^{-3} °K. The expulsion of entropy from the vibrating Casimir Electrode is negligible. We note that simply half of this expended heat occurs in the "go", the second part occurs in the "return" phases of the vibration.

During a cycle from z_0 to z_1, to deform the elastic piezoelectric bridge during the displacement " go " of the vibration , the quantum energy ECASIMIR , given by the quantum vacuum , is used for four different energies:
1/ The mechanical energy for the deformation of the elastic bridge: W_{DEFCA}
2/ The energy to create the fixed Q_F charges in this piezoelectric structure : W_{BRIDGE}

3/ The energy for the simple displacement of the point of application of the Casimir force in the middle of the bridge : $W_{CASIMIR}$
4/ The expulsion of entropy ΔS/2 energy, expended in heat due to the friction of the atoms in the half of the vibration of the bridge heat : $\Delta Q_{vib}/2$

We can write that to deform the piezoelectric bridge from the start position z0 to the position z_1 :

$E_{CASIMIR1} = W_{DEFCA1} + W_{BRIDGE1} + W_{CASIMIR1} + Q_{vib}/2$, (Eq 8).

This quantum vacuum energy $E_{CASIMIR1}$ is bigger than the simple translation energy $W_{CASIMIR1}$. The energies W_{DEFCA} and WBRIDGE are store in the deformed piezoelectric bridge as a potential energy.

1/ The translation energy of the Casimir force is:

$$W_{CASIMIR1} = \int_{z_0}^{z_1} F_{CA}\, dz = \int_{z_0}^{z_1} S\ \frac{\pi^2\ \hbar\ c}{240\ z_s^4} dz_S = S\left(\frac{\pi^2\ \hbar\ c}{720}\right)\left[\frac{1}{z_1^3} - \frac{1}{z_0^3}\right].(\text{Eq } 19)$$

The $W_{CASIMIR1}$ energy represents the translation of the Casimir force F_{CA} from z_0 to z_1 without considering that this force also deforms an elastic and piezoelectric structure from z_0 to z_1. Now, let's calculate the deformation energy W_{DEFCA} of the piezoelectric bridge fixed at both ends.

We know that the deformation energy of an elastic system is the energy that accumulates in the solid body during its elastic deformation. Yet, all Material Resistance book says that the deformation energy W_d of an embedded elastic bridge and for a constant force F is : W_d= ½ z_e F with $z_e = z_0 - z_s$, the deflection (arrow) acquired by the elastic bridge subjected to the constant force F . In the case of our piezoelectric bride the force F being the Casimir force, varies in $1/z^4$, with the distance z.

So, for a differential deflection dz of the bridge under the force F(z) we can write

$$d(W_d) = 1/2\ F(z)\ dz\ . \Longrightarrow W_d = \frac{1}{2}\ W_{DFCA}(z_s) = \frac{1}{2} S\ \frac{\pi^2\ \hbar\ c}{240} \int_{z_0}^{z_1} \frac{1}{z^4}\ dz\ = \frac{1}{6}\ S\ \frac{\pi^2\ \hbar\ c}{240}\left[\frac{1}{z_1^3} - \frac{1}{z_0^3}\right]\ (\text{Eq. } 20)$$

This energy WDEFCA is stored in the elastic bridge as a potential energy and will be used with the energy of a Coulomb's force plus a kinetic energy of all the structure to redress the piezoelectric bridge . The position of the mobile Casimir electrode reaches the limit z_1 when the grid voltage V_G on switch n°1 reaches its threshold voltage VT1 . This reached position z_1 is unstable because the Casimir force increases with its position. As a result, the mobile Casimir electrode can collapse. But, when the Casimir electrode is in position z_1 , the switch n°1 switches to ON . The charges present on the metallic face n°1 of the piezoelectric bridge must homogenize with the metallic Coulomb electrode, which was previously grounded by the closing of switch n°2 . Note that, when switch n°1 switches, switch n°2 is still open because the voltage of the TFT MOS of switch n°2 are in depletion $V_G > V_{T2}$ (Figure 1,4,5,6).

The energy stored in the bridge through its deformation is in z_1 $W_{DFCA1} = \frac{1}{6}\ S\ \frac{\pi^2\ \hbar\ c}{240}\left[\frac{1}{z_1^3} - \frac{1}{z_0^3}\right]$ Eq 21, At position z_2 of the structure, the memorized elastic energy is $W_{DFCA2} = \frac{1}{6}\ S\ \frac{\pi^2\ \hbar\ c}{240}\left[\frac{1}{z_2^3} - \frac{1}{z_0^3}\right]$Eq22 .

We notice that $W_{DEFCA} > 0$ and that the numerical value of WDEFCA1 is a little smaller than the expression calculated when $F_{CA}(z_1)$ was constant : Wd= ½ ze*$F_{CA}(z_1)$.

2/ During the displacement " go " the energy ECASIMIR is also used to generate a potential energy W_{BRIDGE} accumulated in the capacity of this piezoelectric bridge which follows the equation: $d(W_{BRIDGE}) = Q_F\ d(V_{PIEZO})$ with VPIEZO = Voltage between the two metallic faces of the piezoelectric bridge , with $Q_F = C^{PIEZO}\ V_{PIEZO} \Rightarrow W_{BRIDGE1}$ = potential energy at the position z_1

$$W_{BRIDGE1} = \int_0^{Q_1} \frac{Q_F}{C_{PIEZO}}\ d(Q_F) = \left[\frac{Q_F^2}{2\ C_{PIEZO}}\right]_0^{Q_1} = \frac{a_P}{2\ l_P b_P \epsilon_0\ \varepsilon_{PIEZO}} \left(\frac{d_{31}\ l_p}{2\ a_P}\right)^2 F_{CA}^2 =$$
$$\left(\frac{a_P}{2\ l_P b_P \epsilon_0\ \varepsilon_{PIEZO}}\right) \left(\frac{d_{31}\ l_p\ l_s b_s\ \pi^2 c\ \hbar}{480\ a_P}\right)^2 \left[\frac{1}{z_1^4} - \frac{1}{z_0^4}\right]^2 \text{Eq. } (23)$$

We notice that $W_{BRIDGE1} > 0$, similarly when the structure reaches position z_2 , the same memorized elastic energy occurs . To get $W_{BRIDGE2}$ for position z_2 of the bridge, we simply swap z_1 for z_2. In these equations, we use $d(Q_F) = C_{PIEZO}\ d(V_{PIEZO})$, with C_{PIEZO} = electrical capacity of the piezoelectric bridge, $C_{PIEZO}\ \frac{\epsilon_0 \varepsilon_{PIEZO}}{a_P} b_P l_P$ Eq.24 .

We know (Eq2) that the creating fixed charges on this piezoelectric structure is $Q_F = \frac{d_{31} l_P}{a_P} F_{CA}$.

We have Q_e = - Q_F = the accumulated mobile charges, coming from the mass, on the surface of the metallic film. This part W_{BRIDGE} of $E_{CASIMIR}$ is stored in the piezoelectric bridge as potential energy and contributes to the usable energy WELECTRIC appearing during a cycle.So, during the phase "go" from z_0 to z_1 the total energy coming from the vacuum = $E_{CASIMIR}$ is used:
1/to deform the piezoelectric bridge W_{DEFCA},
2/ to produce the electrical charges as potential energy $W_{BRIDGE1}$,
3/Translate the point of application of the Casimir Force $W_{CASIMIR}$,
4/ produce a heat of the structure by the entropic transfer ΔQ_{vib} /2 .

We have:
Energy produces by vacuum = $\mathbf{E_{VACUUM} = W_{DFCA} + W_{CASIMIR} + W_{BRIDGE} + \Delta Q_{vib}/2 = WGOING}$ (Eq 25) WDEFCA and W_{BRIDGE} are potential energies that will be used when the elastic bridge returns to its equilibrium position, that is to say without deformation.

MEMS energy balance during the "return" phase from z_0 to z_1" ,switch n°1 ON, Switch n°2 OFF: 0 < abs (V_{T2}) < V_G < =abs (V_{T1}). and Ratio F_{CO} / F_{CA} > = p: (Figure 1)

Figure 15 page 10 above, shows the F_{CO} / F_{CA} ratio obtained by the choice - defined during the technological realization of the MEMS- of the threshold voltage VT1 of switch n°1. Now , the voltage on the grids of switch n°1 exceed its threshold voltage and switch commute ON. The switch n°2 is till OFF, so the Coulomb's electrode is opened . The free charges Q_{m1}, stored on the metal electrodes of face 1(Fig 1,4 ,5), passing through one of the MOSE transistors, are uniformly distributed on the Coulomb metal electrode of the surface for example S_{C1} = lp*bp. If S_{C1} = S_{P1} , this metallic Coulomb's electrode therefore has approximately a mobile charge Q_{mn} S_{C1}/ S_{P1} = Q_{mn}/2.

This homogenization is obligatory because there is no electric field in a perfect metallic conductor. The free charges Q_{m2}, stored on face 2 and on all the isolated grids TFT MOS don't move. So, grids electrode and return electrode have opposite free charge. (Fig 4,5,15). A Coulomb force FCO then appears between these two electrodes during the very short time when switch no. 2 is still open, isolating the Coulomb electrode from the ground. The resulting force F_R= F_{CO} - F_{CA} is now applied to the piezoelectric bridge. This force F_R, is opposite to the force F_{CA} or null. In presence of this force F_R the deformations of the bridge and its electrical charges, so the grids voltaged are necessarily reduced. Since the threshold voltage V_{T2} of switch n°2 is lower but very close to V_{T1} (we choice V_{T1} – V_{T2} = 50 mV), the time duration during which this Coulomb force is exerted is very small (a few nanoseconds).

Very quickly, the switch n°2 commutes from OFF to ON, grounding the Coulomb electrode via an R.L.C. circuit, (Fig 23). The Coulomb force vanishes quickly after its appearance at position z_2. The values of V_{T2} and V_{T1} impose that z_2 is very close to z_1. So , the energy $W_{COULOMB} = \int_{z_1}^{z_2} F_{CO} dz$ expended by the Coulomb force remains low, even if this force is several times that of Casimir in intensity.

The time of existence of F_{CO} is of the order of a few tens of nanoseconds (fig 1,5). The position z_1 of appearance of this force F_{CO} is such that F_{CO} = p F_{CA} and is numerically calculated by MATLAB(Figure 18)

$$F_{CO}=pF_{CA} \Rightarrow \frac{Q_F\ Q_F}{8\,\pi\,\varepsilon_0\,\varepsilon_r}\left(\frac{1}{z_r+z_0-z_S}\right)^2 = \left[\frac{d_{31}\,l_p}{a_p} S_S \frac{\pi^2\,c\,\hbar}{240}\left(\frac{1}{z_S^4}-\frac{1}{z_0^4}\right)\right]^2 \left(\frac{1}{8\,\pi\,\varepsilon_0\,\varepsilon_r}\right)\left(\frac{1}{z_r+z_0-z_S}\right)^2 = p\,S\,\frac{\pi^2\,c\,\hbar}{240\,z_S^4} \quad \text{Eq 26 .}$$

We note that the position z_1 depends on the values of the interface's z_o of Casimir's electrodes and of Coulomb's electrodes z_r.

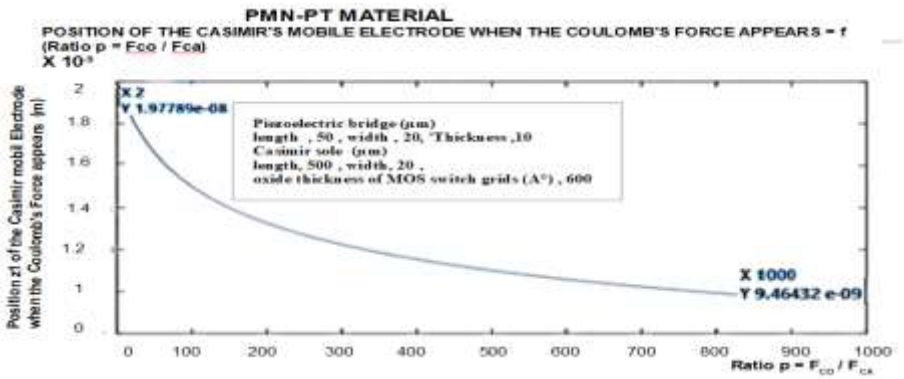

Figure 18: Position of the mobile Casimir electrode z_1 where the Coulomb force occurs : z_r = z_0 =200A°, ls = 500 µm, bs = 20 µm, lp = 50 µm, bp =20µm, ap = 10µm

The $F_R = F_{CO} - F_{CA}$ force is now applied to the mobile structure. This resulting force is at least zero or has a greater intensity than the Casimir force F_{CA}. It contributes with the energy stored in the elastic bridge to straighten the structure and to give it kinetic energy. This FCO force exists as long as switch n°2 has not switched to ground, canceling its existence by the dispersion of charges on the Coulomb electrode. We describe below the energy dispensed in the cycle of the piezoelectric bridge positions. We hope show that a usable energy WELECTRIC is possible and not due to any electrical energy applied but by the dissipation of the mobile electric charges to the mass throw the switch n°2 and an R.L.C. circuit. (Figure 21)

There are two phases for this return to from z_1 to z_0 (returning phase):
1/from z_1 to z_2 where the Coulomb's force F_{CO} exist and contribute to straighten the elastic structure and to give it kinetic energy ,
2/ from z_2 to z_0 where this acquired kinetic energy, and the remaining energy still stored in the structure which will be dissipated by the energy spent by the Casimir force.

Calculation of energies between z_1 and z_2

As soon as switch n°1 has switched to homogenize the electric charges between face 1 of the bridge and the Coulomb electrode, the resulting force $F_{CO} - F_{CA}$ straightens this bridge and the electric charges drop. The electric voltage on the grids falls below the threshold voltage of this switch n°1 which commute again very quickly. The energy $W_{COULOMB}$ is write $W_{COULOMB} = W_{FC0} = \int_{Z_2}^{Z_1} F_{C0}\, dz = \left\{S_S \cdot \frac{\pi^2 \hbar\, c}{240} \cdot \frac{d_{31}\, l_p}{a_p}\right\}^2 \left(\frac{1}{8\,\pi\epsilon_0\,\epsilon_r}\right) \cdot \int_{Z_2}^{Z_1} \left[\left(\frac{1}{z_s^4} - \frac{1}{z_0^4}\right)\left(\frac{1}{z_r + z_0 - z_s}\right)\right]^2 dz_s$ Eq27 . This energy exists only between the very close positions z_1 and z_2. The literal formulation of $W_{COULOMB}$ energy is possible but its expression is not convenient because it is too complex. We prefer to calculate by MATLAB its numerical value between the value z_1 and z_2.

The position z_2 of commutation of switch n°2 is deduced from the chosen threshold value V_{T2} of switch n°2.
We note that we can minimize the value of the energy spent by WCOULOMB, by choosing a value of the threshold voltage V_{T2} close but slightly lower than V_{T1} of switch n°1.For example $V_{T2} = V_{T1} - 0.05$ (V). We use MATLAB to find position z_2 of commutation of circuit 2 to cancel the Coulomb's Force F_{CO}, see (Eq 22) and figure 18. We have, at position z_2 of the bridge, the electric charge in the TFT MOS .

$$Q_2 = \frac{d_{31}\, l_p}{a_p}\, S_S\, \frac{\pi^2\, c\, \hbar}{240} \left(\frac{1}{z_2^4} - \frac{1}{z_0^4}\right) \text{ with } Q_2 = Cox\, V_{T2} \text{ So }, z_2 = \frac{1}{\sqrt[4]{\left[\frac{240\, a_p\, C_{ox}}{d_{31}\, l_p\, \pi^2\, c\, \hbar\, S_S} V_{T2} + \frac{1}{z_0^4}\right]}} \quad \text{(Eq .28).}$$

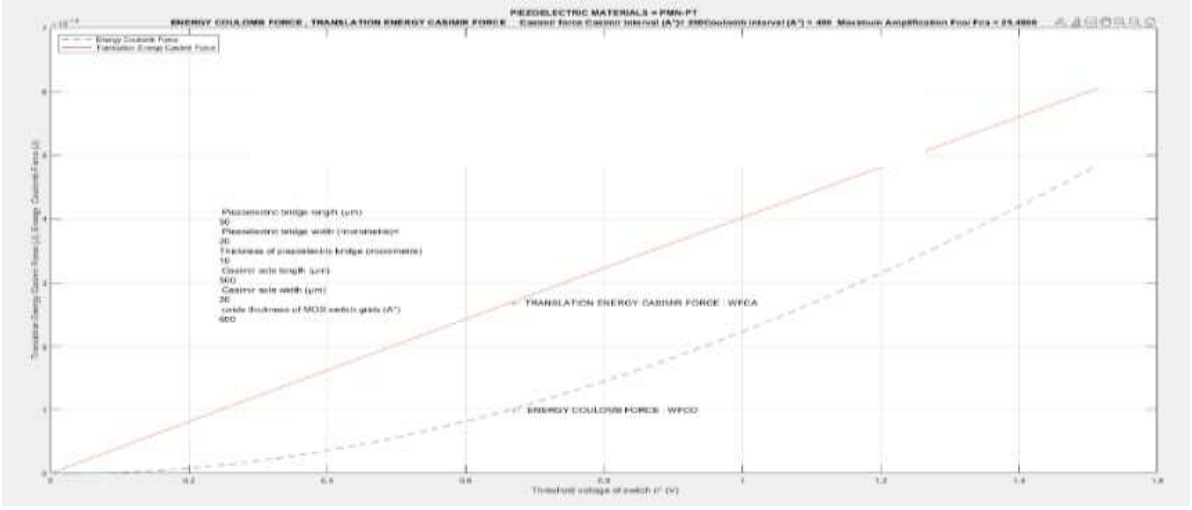

Figure 19: Energy of translation of Casimir Force and energy of Coulombs 'Force between its apparition in the position z_1 and its disappearance in position z_2

We present in figure 21 the curve representing the translation energy of the Casimir force as well as the Coulombs force the time when the structure is between the positions z and z, which represents a few nanoseconds.

We can calculate the energy spent in the first part of return of the structure (from z_1 to z_2) Figure 6 , by simply calculating the kinetic energy WCIN acquired by the structure when it reaches the position z_2 upon its return . We know that the variation of the kinetic energy W_{CIN} is equal to the sum of all the energies supplied or spent on the moving structure. Thus, as we know the numerical value of all these participants in the variation of this kinetic energy W_{CIN}, we can write equation Eq.25 which allows us to calculate W_{CIN} because all the terms of this equation are known.

$$W_{CIN} = (W_{DFCA1} + W_{BRIDGE1}) - (W_{DFCA2} + W_{BRIDGE2}) + W_{COULOMB} - (W_{CASIMIR1} - W_{CASIMIR2})$$ (Eq. 29) and fig 20.

All the terms of equation are known , so we know now the kinetic energy acquired by all the mobile system in z1 and know when the Coulomb force disappears. All calculations done, we obtain :

$$W_{CIN} = \frac{1}{6} S \frac{\pi^2 \hbar c}{240} \left(\frac{1}{z_2^3} - \frac{1}{z_1^3}\right) + W_{COULOMB}$$

We know now the kinetic energy acquired in z_1 and know when the Coulomb force disappears.
The structure must now spend this energy which gives it inertia. The braking energy provided by the Casimir force will cancel this kinetic inertia plus that stored in the elastic energy. Let us calculate the final ascent position z_f of the mobile structure. It has an inertia provided by the kinetic energy WCIN, a stored elastic energy WDFCA but is slowed down by the energy provided by the Casimir force.

$$\text{We can write } W_{CIN} + \frac{1}{6} S \frac{\pi^2 \hbar c}{240} \left(\frac{1}{z_2^3} - \frac{1}{z_f^3}\right) = \frac{1}{3} S \frac{\pi^2 \hbar c}{240} \left(\frac{1}{z_2^3} - \frac{1}{z_f^3}\right) \Rightarrow W_{CIN} = \frac{1}{6} S \frac{\pi^2 \hbar c}{240} \left(\frac{1}{z_2^3} - \frac{1}{z_f^3}\right)$$

We deduce of this equation that the final position zf of the bridge is $z_f = \frac{1}{\sqrt[3]{\left[\frac{1}{z_2^3} - \frac{1440\, W_{CIN}}{\pi^2 \hbar c}\right]}}$ Eq 30 .

We can see in Figure 22 that depending on the acquired inertia, which depends on the energy provided by the Coulomb force, zf can slightly exceed its initial position. We will use this property at the end of this article in order to increase usable energy.

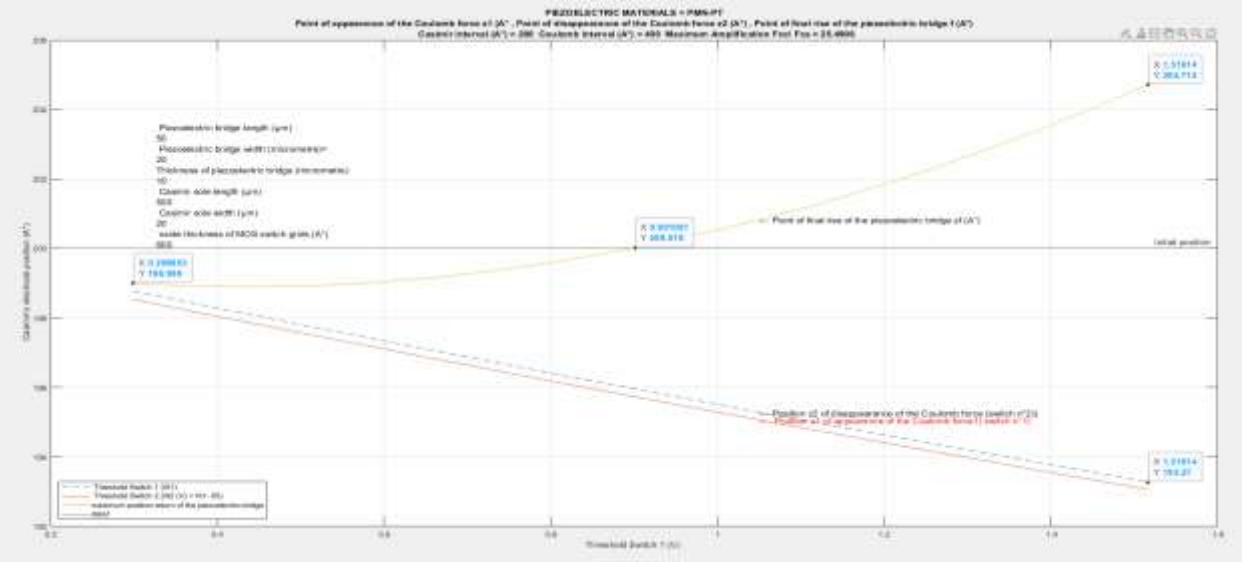

Figure 20: Positions of : 1/ The final rise z_f of the structure, 2/ of the point z_2 of disappearance of the Coulomb force depending on the threshold voltage V_{T2} of switch n°2, 3/ of the point z_1 of appearance of the Coulomb force depending on the threshold voltage V_{T1} chosen for switch n°1

It is easy to calculate the damping energy $W_{CASIMIR2}$ that appears between the intermediate position z_2 and the final position z_f. We have $W_{CASIMIR2} = \int_{z_2}^{z_f} F_{CA}\, dz = \int_{z_2}^{z_f} S \frac{\pi^2 \hbar c}{240\, z_s^4} dz_S = S\left(\frac{\pi^2 \hbar c}{720}\right)\left[\frac{1}{z_f^3} - \frac{1}{z_2^3}\right]$ (Eq 31)

As, at position z_2 the switch n° 2 commutes to ON and puts the Coulomb electrode to ground through the RLC circuit below (Fig 21) . The electrical charges present on the Coulombs electrode flow towards the ground, creating a current and a power which remains to be evaluated.

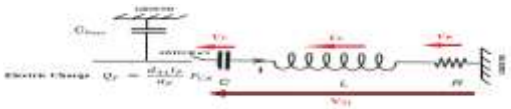

Figure 21 : RLC circuit to power the autonomous electronics for converting power peaks into direct voltage

We now evaluate this usable current flowing to ground. We put in the circuit, an adjustment capacitance C in series with C_{PIEZO}. We call $C_E = \frac{C_{PIEZO}\, C}{C_{PIEZO} + C}$ the equivalent capacity of the two capacities in series. When the switch n°2 commutes, we have the equation $U_C + U_L + U_R = C_{PIEZO} / Q_F = V_{T1}$ (Figure 21) , with $U_R = R\, I$, $U_L = L\, dI/dt$ and $Q_F = U_C\, C_{PIEZO}$. With R representing resistance, L denoting inductance, and C indicating capacitance. After rearranging we have the following equation $\frac{d^2 U_C}{dt^2} + \frac{R}{L}\frac{dU_C}{dt} + \frac{U_C}{L\,C} = 0$ Eq 32.

This differential equation has solutions that depend on the value of its determinant. We choose the values of R, L, C in such a way that the determinant $\Delta = \sqrt{\left(\frac{R}{L}\right)^2 - \frac{4}{LC}} = 0$ of this equation is positive or vanishes. So, if Δ = 0 the solution is : $x_1 = \frac{R}{2\,L}\left(-1 + \sqrt{1 - \frac{4\,L}{C\,R^2}}\right) = -\frac{R}{2\,L}$ and $x_2 = \frac{R}{2\,L}\left(-1 - \sqrt{1 - \frac{4\,L}{C\,R^2}}\right) = -\frac{R}{2\,L}$ then we have $x_1 = x_2 = -\frac{R}{2\,L}. < 0$

Considering the initial conditions, we obtain

$u_c = \frac{V_{T1}}{x_1 - x_2}\,[x_1 \exp(x_2 t) - x_2 \exp(x_1 t)]$ Eq 33, $i_c = C\frac{du_C}{dt} = C\frac{V_{T1}\; x_1 x_2}{x_1 - x_2}\,[\exp(x_2 t) - \exp(x_1 t)]$Eq34 The peak of current is given when $d(i_c)/dt = 0$ so at the time $t_{imax} = \frac{Ln\left(\frac{x_2}{x_1}\right)}{x_1 - x_2} = \frac{Ln\left(\frac{1 + \sqrt{1 - \frac{4\,L}{C\,R^2}}}{1 - \sqrt{1 - \frac{4\,L}{C\,R^2}}}\right)}{\frac{R}{L}\sqrt{1 - \frac{4\,L}{C\,R^2}}}$ Eq 35 Replacing t by t_{imax} in the equation 33 and 34 we obtain the expression for the maximum of the voltage is $u_{cmax} = V_{T1}$ and of the maximum current i_{cmax} ;

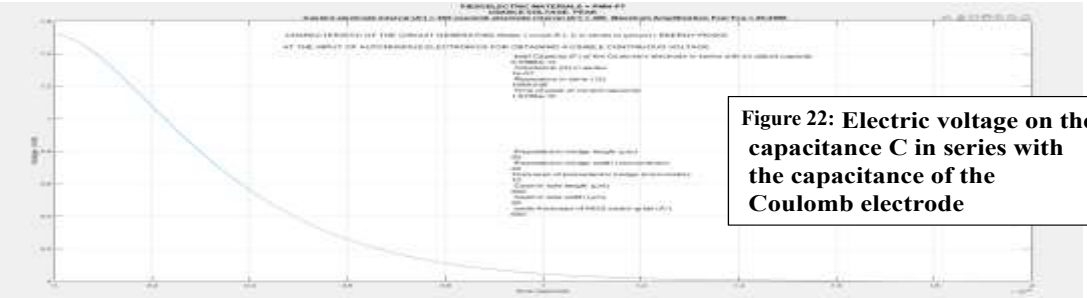

Figure 22: Electric voltage on the capacitance C in series with the capacitance of the Coulomb electrode

Figure 22 : Electric voltage on the capacitance C in series with the capacitance of the Coulomb electrode

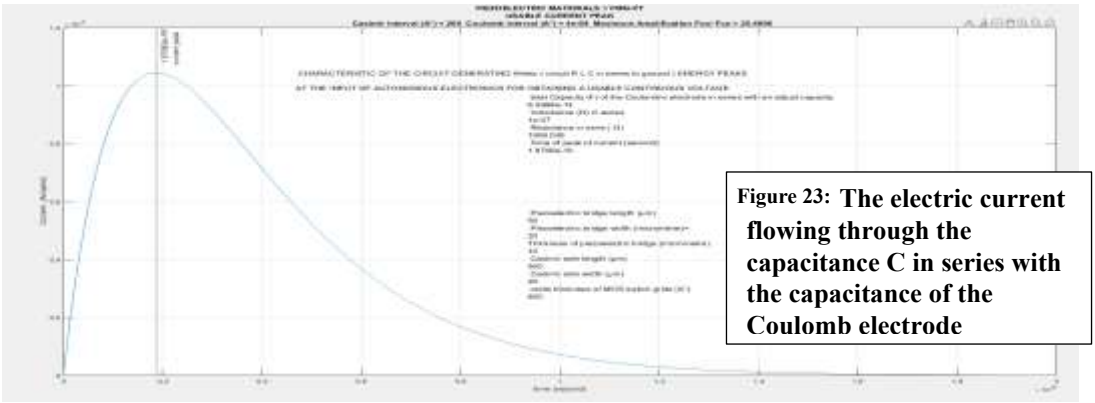

Figure 23: The electric current flowing through the capacitance C in series with the capacitance of the Coulomb electrode

The electrical power of the signal is :

$P(t) = u_c\, i_c = \left(\frac{V_{T1}}{x_1 - x_2}\right)^2 C\, x_1 x_2\,[\exp(x_2 t) - \exp(x_1 t)][x_1 \exp(x_2 t) - x_2 \exp(x_1 t)]$ Eq36

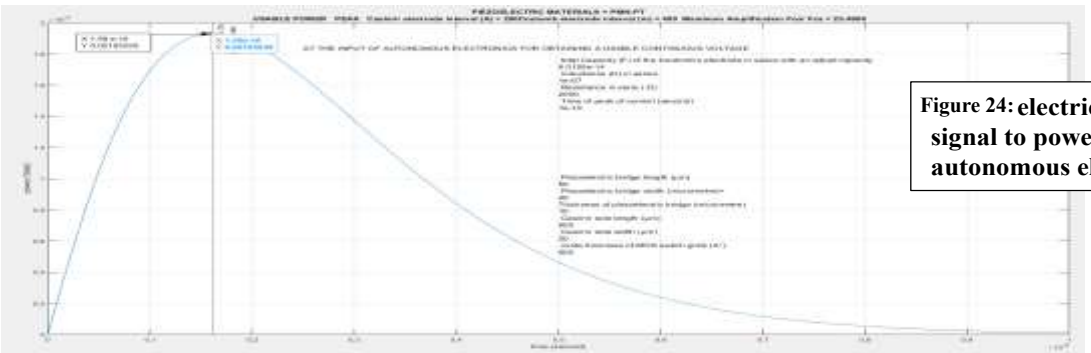

Figure 24: electrical power of the signal to power the autonomous electronics

We note on Fig 23 and 24 that the maximum t_{imax} = 1.87 10^{-10} (s) for the peak current is different than those t_{pmax} = 3.03 10^{-10} for the peak power P(t) The peak power of 1.93 mW is sufficient to power the autonomous electronics of fig 18,19 and obtain a useful voltage of several volts in a few milliseconds. The period of a vibration being (fig 10) of 0.2 µs for an F_{CO} /F_{CA} of simply 2, the average power over a period is then approximately ≈ 0.3 µW.

We deduce that the power provided by the system in 1 second is of the order of 3e-7 / 2e^{-7} ≈ 1.5 W.

Knowing the electrical power P(time) we can numerically evaluate this finale and useable energy, by MATLAB. We obtain $W_{ELECTRIC}$ in fig 27 .

$$W_{ELECTRIC}(t) = \int_0^{10*t_{max}} u_c\, i_c\, dt = \left(\frac{V_{T1}}{x_1 - x_2}\right)^2 C\, x_1 x_2 \int_0^{10*t_{max}} [\exp(x_2 t) - \exp(x_1 t)][x_1 \exp(x_2 t) - x_2 \exp(x_1 t)]\, dt \quad \text{Eq37}$$

The energy balance is completed for the "return" phase to its initial position of the structure.

We have $\mathbf{W_{RETURNING} = W_{CIN} + W_{ELECTRIC} + W_{DFCA2} + W_{BRIDGE2} - W_{CASIMIR2} + \Delta Q_{vib}/2}$ **(Eq 38)**

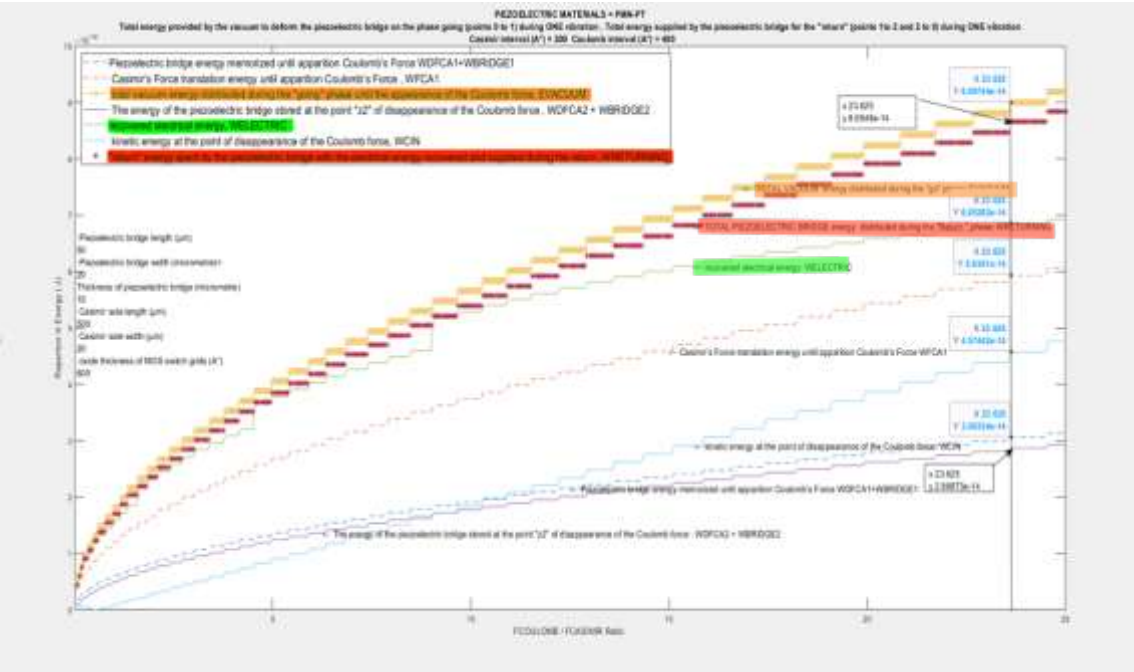

Figure 25: Balance of the energies of the "go" and "return" phases for the proposed MEMS which seems to be able to "extract energy from the quantum vacuum."

With Figure 25, we can make the energy balance of the energy sources provided by the quantum vacuum in the "going" and "returning" phases. The constant energy provided by the quantum vacuum ocean in the "go" phase simply changes its nature and subdivides into other energies in the "return" phase of vibrations. One of these energies in this "return" phase can be used by creating a little electrical energy. We note that the energy necessary for the perpetual maintenance of these vibrations is constantly provided by the isotropic and timeless energy of the quantum vacuum and that it is possible to extract from this gigantic ocean of energy of "nothing" a small electrical and exploitable energy. Whatever the F_{CO}/F_{CA} amplification factor, we note that WRETURNING is always slightly lower than E_{VACUUM} , thanks to the choice of $W_{ELECTRIC}$

We observed that in the referential of our 4 dimensions Space-Time plus the Quantic Vacuum, the energy is conserved which is consistent with Noether's theorem.This very important theorem of 1905 explains why, as Monsieur de Lavoisier said, "Nothing is created, nothing is lost, everything is transformed.".

Remember that energy is defined as the "physical quantity that is conserved during any transformation of an isolated system. However, the system constituted by simply the MEMS device in space is not an isolated system while the system constituted by the MEMS device plus the space plus the energy vacuum seems an isolated system. The part of the MEMS energy sensor vibrates at frequencies depending on the size of the structure and operating conditions, but with an amplitude of just a few Angstroms. These vibrations aren't perpetual motion; they can be continuously powered by vacuum energy from the Casimir force.

The following diagram summarizes the operation of this presented MEMS (Figure 26 and Figure 27)

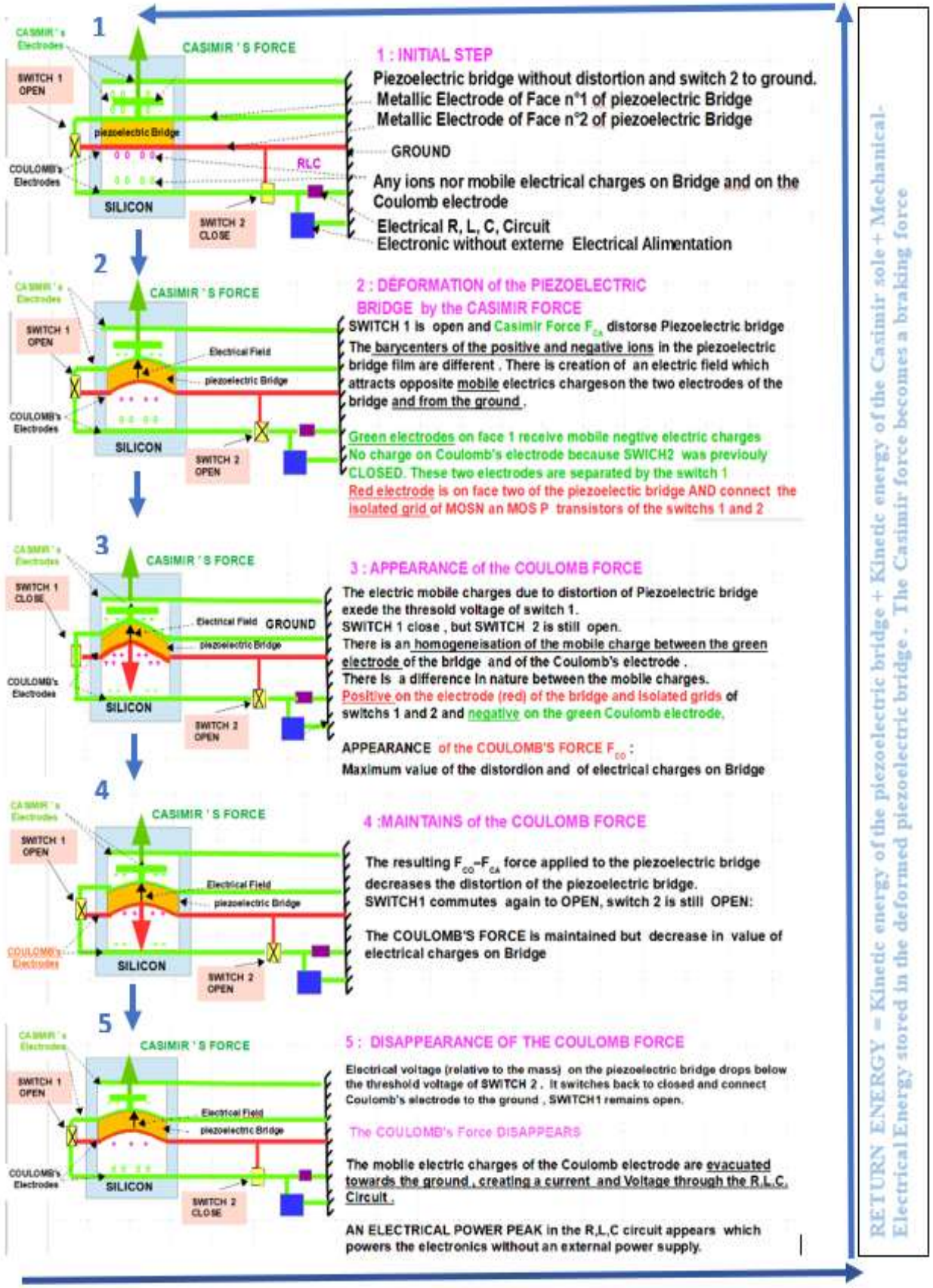

Figure 26: Overview of the 5 successive and repetitive steps of the M.E.M.S.

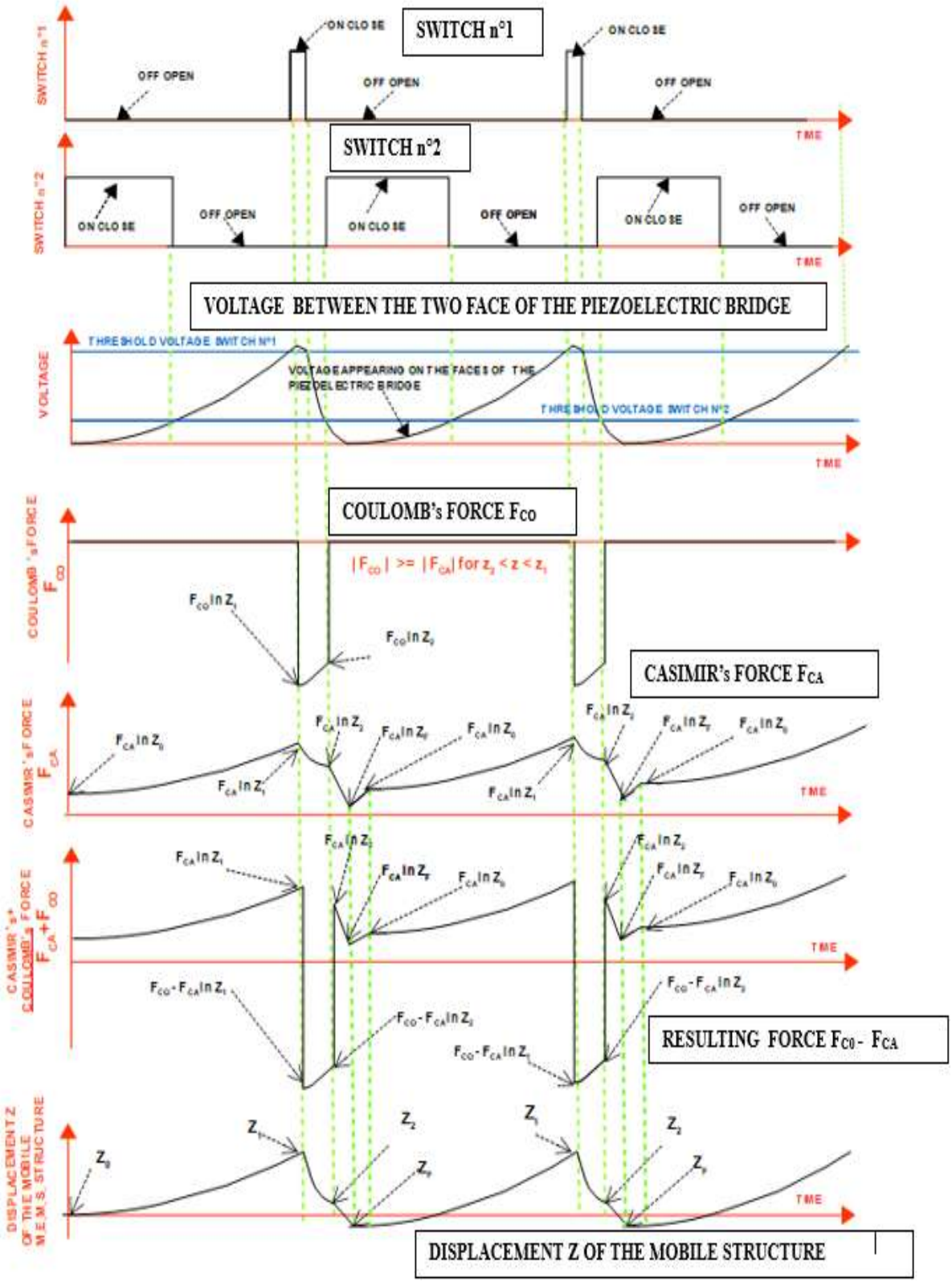

Figure 27: shape of the curves representing 1/ The switching of the two switches 2/ The electrical voltage on face 1 of the piezoelectric bridge 3/ The Casimir forces F_{CA} 4/ The coulomb forces F_{CO} 5/ the energies W_{FCO}, W_{FCA} , W_{FCO} -W_{FCA} 6/ The maximum elevation zf of the moving part

We notice in the previous pages that the piezoelectric bridge could reach a position z_f which exceeds its initial position z_0. We can take advantage of this observation by modifying the moving part of this MEMS to provide the RLC ccircuit with the two signs of current peak and voltage emitted by the sensor. This modification should increase the continuous electrical voltage on the capacitive output of the autonomous electronic circuit whose role is to transform the signals from the quantum vacuum energy sensor (Figure 28)

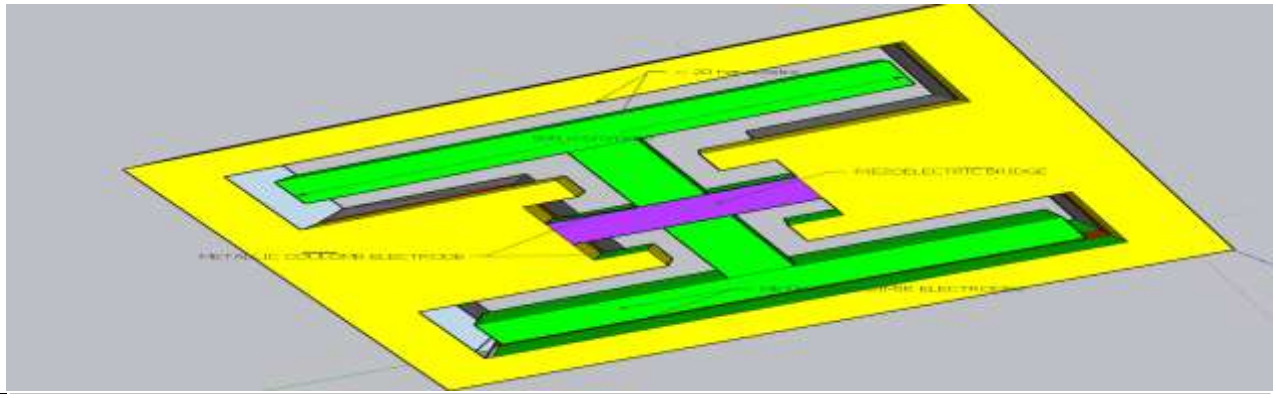

Figure 28: Shape of the MEMS circuit making it possible to double the direct voltage at the output of the autonomous electronic circuit, by providing it with consecutive voltage and current peaks of opposite sign.

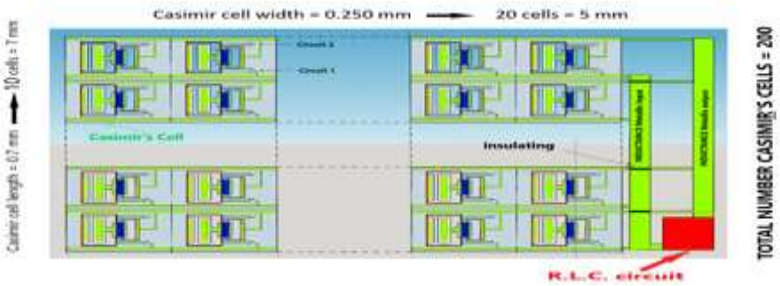

Figure 29: Positioning of 20 Casimir cells in parallel and 10 in series. Total of Casimir cells delivering a periodic current during a small part of the vibration frequency of the devices = 200. Total des cellules = 200, Width = 5mm, Length = 7 mm

In order to obtain a current peak greater in intensity, the Casimir cells can be positioned in a series and parallel network at the 2 terminals of a single and as described RLC circuit for example, 20 Casimir cells can be placed in parallel and 10 in series ,(Figure 29).Important increase in current intensity, time duration of the peak, as of the voltage peak .This work on the energy balance of a M.E.M.S., which appears to be able to extract energy from a new, totally unexploited source, was carried out completely alone and without the help of any organization, by an old retiree. It seems that - unless there is always a possible error - the fundamental theorem of EMMY NOETHER from 1905 is not contradicted. In the event of a theoretical confirmation by specialists, the supreme and definitive judgement will be the realization of a prototype, and I will be happy to participate in this development

Autonomous electronics to transform the cyclic power peaks from the R.L.C circuit

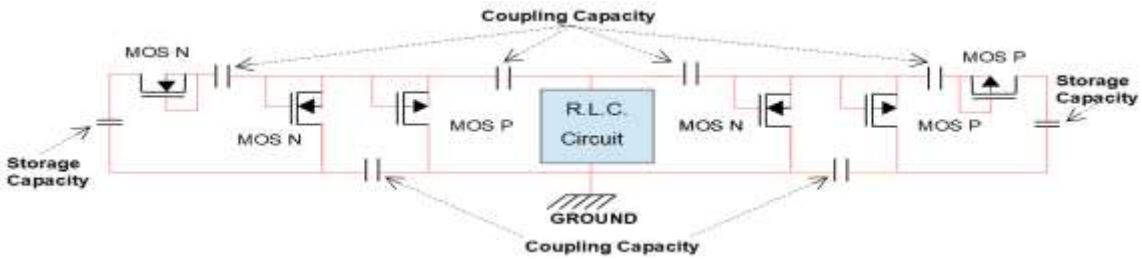

Figure 30: Principle of the single-stage doubler without power supply electrical diagram. All the MOS are isolated from each other by etching on an S.O.I wafer, and their threshold voltage is as close as possible to ground

The circuit of the figure 30 is an autonomous device operating without any electrical power source. It rectifies and accumulates the repetitive peak power delivered to the terminals of the RLC circuit in the figure 4 and 5 and transforms them into a usable direct voltage source. The impedance of the output of this autonomous circuit must be important .

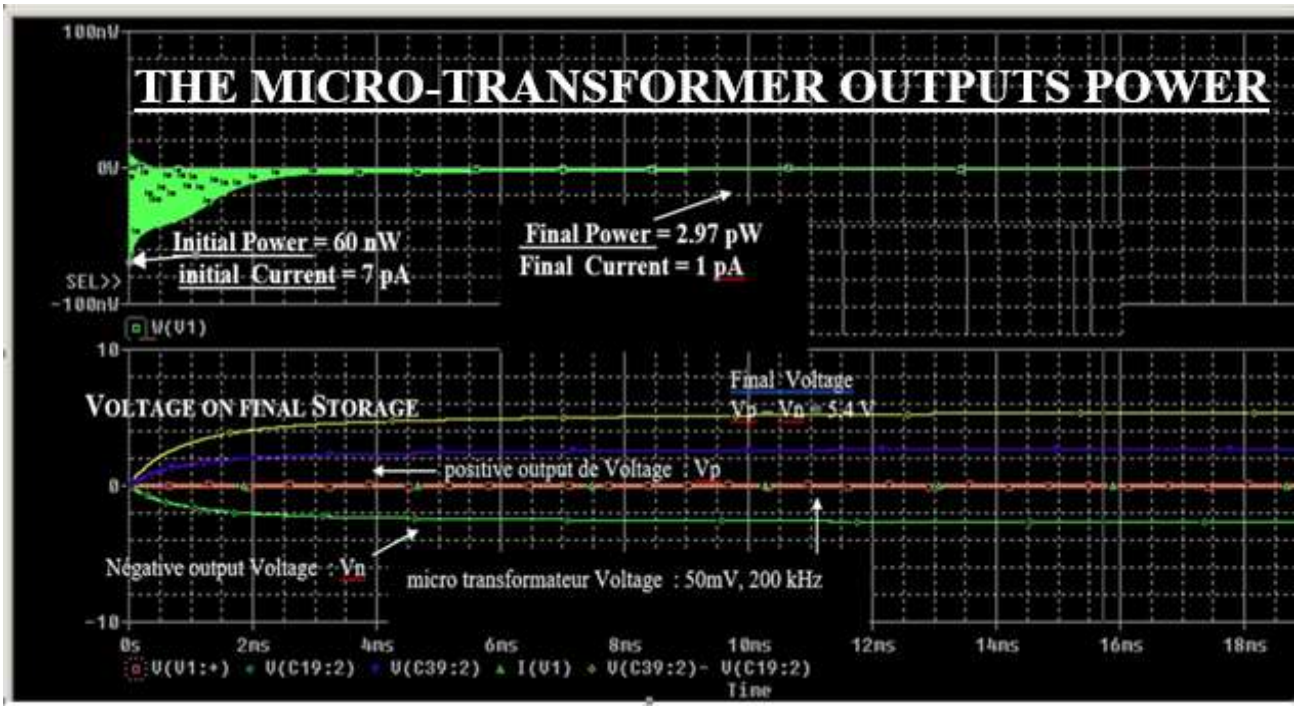

Figure 31: SPICE simulations of voltages, current, power consumed by the autonomous electronics for the transformation into direct voltage (5.4 V) of an alternating input signal of 50 mV, frequency = 150 kHz, number of stages = 14, coupling capacities = 20 pF, storage capacity = 10 nF.

We note the extreme weakness of the electrical power required at the start of the conversion of the power peaks (60 nW) and at the end (2 pW). This transformation requires 4 ms .

CHARACTERISTICS OF OUTPUT VOLTAGES (V), POWERS (nW) CURRENTS (nA)
AS A FUNCTION OF THE NUMBER OF STAGES
INPUT SIGNAL FREQUENCY = 150 kHz OUTPUT VOLTAGE MEASUREMENT FOR t = 50 ms

	Vg=50mV					Vg=100mV				
number of stages	Output Voltage	Current (nA) start	Current (nA) end	Power (nW) start	Power (nW) end	Output Voltage	Current (nA) start	Current (nA) end	Power (nW) start	Power (nW) end
2*3	550mV	300nA	26nA	15nW	1.3nW	1.1v	800nA	46nA	75nW	5nW
2*6	1	300nA	29nA	13nW	1.3nW	2V	700nA	67nA	60nW	6.5nW
2*14	2.2v	300nA	40nA	14nW	2.6nW	4.5v	700nA	50nA	65nW	4.8nW
2*21	2.8v	250nA	38nA	13nW	860pw	6v	600nA	80nA	60nW	2.7nW
2*30	3.3	250nA	43nA	12nW	1.2nW	6.5V	750nA	85nA	61nW	4nW
2*39	3.5v	250nA	45nA	12nW	900pW	7.5V	750nA	95nA	64nW	3.5nW
2*48	3.6v	250nA	46nA	12nW	1nW	7.6V	750nA	100nA	60nW	4.2nW
2*60	3.8	270nA	47nA	12nW	1.1nW	7.9V	700nA	90nA	65nW	4.2nW
2*61	3.8	270nA	48nA	12.1nW	1.3nW	8V	700nA	90nA	65nW	42nW

Table 1: Output Continuous voltage , with current and power consumed by the autonomous electronic in function of two input cyclic voltage parametrized with the number of stages

The interesting points for the presented electronics' device are:

1 / the low alternative input voltages required to obtain a continuous voltage of several volts at the output
2 / the low power and current consumed by this conversion and amplification circuit on the source which in this case is only R.L.C. circuit, supplied by the current peaks generated by the autonomous vibrations.
3 / the rapid time to reach the DC voltage (a few tens of milliseconds)

The technology used to fabricate the MOSNE and MOSPE transistors with the lowest possible threshold voltages, is CMOS on intrinsic S.O.I. and each element are isolated from each other on independent islands. This technology, represented in the following figure 54, strongly limits the leakage currents.

Figure 31: S.O.I technology for making the elements of the "doubler"

We note that, the coupling capacities of 20 pF of this electronic, like that of storage of the order of 10 nF, have relatively high values. To minimize the size of these capacitors we propose to use of titanium dioxide as insulator, with a relative permittivity of the order of 100 which is one of the most important for a metal oxide, then the size of the capacity passes to 33 µm for a thickness of TiO2 = 500 A °, which is more reasonable.

Technology of realization of the current extractor device using the forces of Casimir in a vacuum

For the structures presented above, the space between the two surfaces of the reflectors must be of the order of 200 A °, …. which is not technologically feasible by engraving. Yet it seems possible to be able to obtain this parallel space of the order of 200 A ° between Casimir reflectors, not by etching layers but by making them thermally grow. Indeed, the SS3 and SS2 surfaces of the Casimir reflector must:

• be metallic to conduct the mobile charges
• insulating as stipulated by the expression of Casimir's law who established for surfaces without charges.
• This should be possible if we grow an insulator on the z direction of the structure, for example Al2O3 or TiO2 or other oxide metal which is previously deposited and in considering the differences in molar mass between the oxides and the original materials.

For example, silicon has a molar mass of 28 g/mol and silicon dioxide SiO2 of 60 g/mol. It is well known that when a silicon dioxide SiO2 grows by one unit, a silicon depth of about 28/60 = 46.6% .This means that the fraction of oxide thickness "below" the initial surface is 46% of the total oxide thickness according to S.M. Sze. [9] The same must happen, for example for thermal growth of alumina. The molecular masses of Alumina and aluminium are M_{Al2O3} = 102 g/mole and M_{Al} = 27 g/mole. We obtain an aluminium attack ratio of 27/102 = 26%, which implies that the original surface of this metal has shifted by 26% so that 74% of the alumina has grown out of the initial surface of the aluminium….

As regards the technological manufacture of electronics and structure, it therefore seems preferable:
1 / For electronics to choose Titanium Oxide because of its high relative permittivity ε_r =114 allowing to minimize the geometries required for the different capacities

2 / For the Casimir structure, the choice of aluminium, because its low density increases the resonant frequency of the structure and that 74% of the Alumina Al2O3 is outside the metal, allowing to reduce the interface between Casimir electrodes. A simple calculation shows for example that for aluminium gives : :

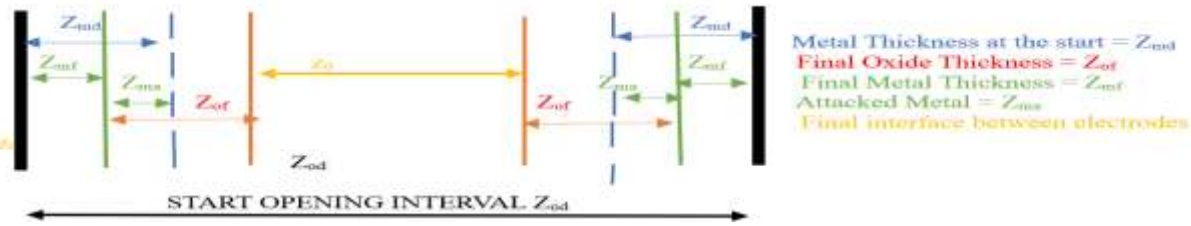

Figure 32: distribution of thicknesses

$z_{od} = 2(z_{md} + z_{of} - z_{ma}) + z_o = 2[z_{md} + (1\text{-}0.26)\, z_{of} + z_o \Rightarrow z = z_{od} - 2(z_{md} + 0.74\, z_{of})$

For example, we start from an opening z_{od} = 3 µm. We deposit a metal layer of aluminium that is etched leaving a width z_{md} = 1 µm on each side of the reflector. Then an Alumina Al_2O_3 can grow, the thickness of which is precisely adjusted, simply by considerations of time, temperature, and pressure to increase a necessary thickness to have the desired interface z0. For example, if z_0 = 200A °, zod = 3 µm, z_{md} = 1 µm, then z_{of} = 0.662 µm. So, we obtain a Casimir interface of 200 A°. The final remaining metal thickness will be z_{mf} = 0.338 µm and will act as a conductor under the aluminium oxide.

Obviously, the growth of this metal oxide between the electrodes of the Casimir reflector modifies the composition of the dielectric present between these electrodes, therefore of the mean relative permittivity of the dielectric. Let: ε_0 be the permittivity of vacuum and ε_0. ε_r the metal oxides one (ε_r = relative permittivity ≡ 8 in the case of Al_2O_3), zof the final oxide thickness on one of the electrodes and z the thickness of the vacuum present between electrode, (initially we want z = z_0).

Then the average permittivity e_{0m} of the dielectric is:

$$\varepsilon_{0m} = \frac{z_{of}\,\varepsilon_0\,\varepsilon_r + z_0\varepsilon_0 + z_{of}\,\varepsilon_0\,\varepsilon_r}{\left(2\,z_{of} + z_0\right)} = \varepsilon_0\,\frac{\left(2\,z_{of}\,\varepsilon_r + z_0\right)}{\left(2\,z_{of} + z_0\right)} \simeq \varepsilon_0\,\varepsilon_r$$, because z_0 is << z_{of}...

For example, z_{of} = 6620 A° is large compared to z <= 200A ° therefore $\varepsilon_{0m} \cong 8 * \varepsilon_0$ in the case of Al_2O_3.

We have considered this change in permittivity in the preceding simulations.

Steps for the realization of the structure and its electronics

We use an SOI wafer with an intrinsic silicon layer : The realisation start with voltage "doubler" is obtained by using CMOS technology with 8 ion implantations on an SOI wafer to make :

1 / The sources, drains of the MOSNE, MOSND of the "doubler" and of the Coulomb force trigger circuits and of the grounding
2 / The source, drains of the MOSPE, MOSPD of the "doubler" and of the Coulomb force trigger circuits
3 / The best adjust the zero-threshold voltage of the MOSNE of the "doubler" circuit
4 / The best adjust the zero-threshold voltage of the MOSPE of the "doubler" circuit
5 / To define the threshold voltage of the MOSNE of the circuit n°1
6 / To define the threshold voltage of the MOSPE of the circuit n°1
7 / To define the threshold voltage of the MOSND of the circuit n°2
8 / to define the MOSPD threshold voltage of the circuit n°2

This electronic done, we take care of the vibrating structure of CASIMIR

9 / engrave the S.O.I. silicon to the oxide to define the location of the Casimir structures (figure 33)

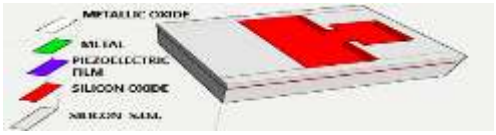

Figure 33 : 9/ etching of S.O.I

10/ Place and engrave a protective metal film on the rear faces of the S.O.I wafer (figure 34)

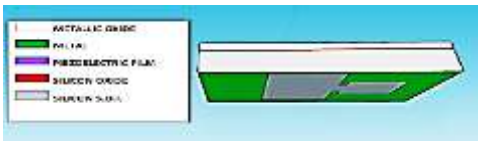

Figure 34: 10/ Engraving of the protective metal rear face of the S.O.I. silicon

11 / Deposit and engrave the piezoelectric layer (figure 35)

Figure35: 11/deposition and etching of the piezoelectric layer deposition and etching of the

12/ Depose and etch the metal layer of aluminium (figure 36) .

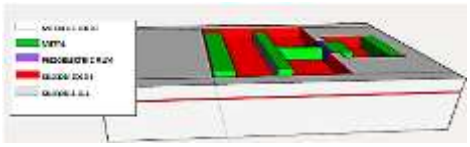

Figure 36: 12/ Metal deposit, Metal engraving etching of the piezoelectric layer

13 / Plasma etching on the rear side the silicon of the Bulk and the oxide of the S.O.I wafer protected by the metal film to free the Casimir structure then very finely clean both sides (figure 37)

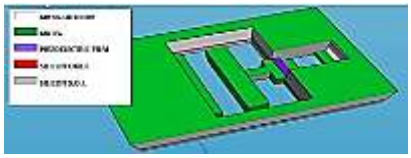

Figure 37: 13/ view of the Casimir device on the rear face, engraving on the rear face of the structures.

After extremely careful cleaning and cutting of the wafer obtained, place it in a support box and proceed to the final oxidation under a temperature lower than 150°C of the entire wafer. The measurement of an adequate voltage obtained at the output of the autonomous transformation electronics indicates that the Casimir and Coulomb effect are effective. This measurement automatically controls the end of the oxidation. Then close the box under neutral gas or vacuum. Thermal oxidation after very fine cleaning of the wafer and at the very end of the process makes it possible to control the thickness of the very fine interface between the Casimir and Coulomb electrodes and to oxidize the cleanest possible surfaces without defects.

14 / Place the structure in a hermetic integrated circuit support box and carry out all the bonding necessary for the structure to function
15 / Achieving thermal growth of aluminum oxide Al_2O_3 or by Atomic Layer Deposition (ALD) at a temperature below 150°C, with measurement and control of the thickness obtained by the packaged circuit. The thickness of the ALD layer is extremely homogeneous. ALD deposition is considered perfectly conformal. Under ideal temperature and pressure conditions, with properly chosen parameters, the chemical reactions are complete, thus leaving no impurities in the coating. The coating is dense and exhibits homogeneous, non-columnar growth. The in situ electronic circuit should generate a measurable electrical signal when the interface between the Casimir electrodes becomes weak enough for the device to vibrate and generate a DC voltage, thereby stopping oxidation or ALD deposition. The electronic circuit should generate a signal when the interface between the Casimir electrodes becomes weak enough for the device to vibrate ... and then stop the oxidation. (Figure 38)

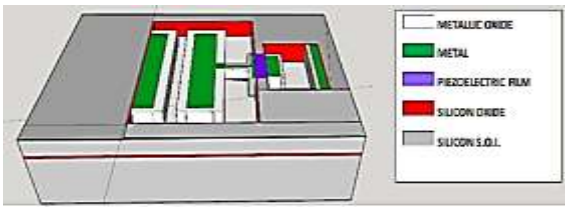

Figure 38:
15 /Adjusted growth of metal oxide front view of the Casimir device and Coulomb's electrode , under automatic electronic control,

16 / Create a vacuum in the hermetic box

In the case where the 2 metal electrodes of Casimir, adhere to one another, they can be separated by the application of an electrical voltage on the Coulomb's electrodes.

• Create a vacuum in the hermetic box

In the case where the 2 metal electrodes of Casimir, adhere to one another, they can be separated by the application of an electrical voltage on the Coulomb's electrodes.

Conclusions and Future Perspectives

This vacuum energy concept was carried out by an old retiree , completely alone and without the help of any organization We observed that in the referential of our 4 dimensions Space-Time plus the Quantic Vacuum, the energy seems to be conserved which is consistent with Noether's theorem and a perpetual small vibration exist.
I say it seems because , in this preliminary work , totally alone , I don't take the time to verify theoretically resume here :
• Neglect of Nonlinearity: The linear dynamic equations do not account for nonlinear electrostatic spring effects or nonlinear material responses, especially at small scales.
• Idealized Joint and Surface Conditions: The assumption of perfect pivoting and mirror-flat Casimir plates does not hold at the nanometer level.
• Unvalidated Mechanical Model: There is no comparison with experimental MEMS resonance data or full 3D FEM models (e.g., from COMSOL or high-fidelity ANSYS simulations).

Piezoelectric Material Selection :
The simulations assume ideal material properties, without accounting for thin-film degradation, surface effects, or substrate interactions. No experimental validation or real deposition results are presented
PZT : Simulations show feasible behavior with moderate output (~10^{-6} to 10^{-4} A). However, PZT is lead-based, raising environmental and manufacturing concerns.

PMN–PT :Shows the highest theoretical performance due to a very high piezoelectric coefficient ($d_{31} \approx 1450$ pC/N). However, film deposition at microscale with preserved d_{31} is technologically nontrivial. The required ~10 μm thick layers are difficult to deposit uniformly while maintaining crystalline orientation and domain structure.

Electrical Conversion Circuit

The energy harvested from the piezo is routed through a MOSFET-controlled switching circuit and then rectified and multiplied using a passive voltage multiplier network. We remark that :

• Efficiency Assumptions: Simulations ignore MOSFET leakage, gate capacitance, threshold variability, and parasitic losses.

• Timing Stability: The concept relies on perfect triggering of MOSFETs based on charge thresholds that are sensitive to temperature and manufacturing variability.

• Lack of Practical Data: No load-line analysis, impedance matching, or power trace simulation is provided. No test circuit is presented or fabricated.

Technological Feasibility

The microfabrication scheme (using SOI wafers, etching, sputtering, etc.) is standard in concept, but several major issues are overlooked:

• Surface Purity: Any contamination layer (organic films) on Casimir plates suppresses the effect significantly.

• Integration Complexity: Combining PMN–PT films, metal contacts, and active electronics on a single substrate with tight thermal and mechanical tolerances might be complex.

• Switching Timing Precision: The exact timing and response of the electrostatic reset stage relies on transistor thresholds differing by as little as tens of millivolts must be validate .

Physical Realism and Fundamental Objections

• Can Vacuum Energy Be Truly Extracted? In mainstream quantum field theory, Casimir energy is a potential well, not a power source. Moving plates into or out of this well costs energy.

• Stability of Oscillations: No analysis of long-term stability, phase noise, or stochastic behavior under vacuum fluctuations is provided.

• Zero-Point Fluctuation Limitations: The model is deterministic and does not account for the inherently probabilistic nature of vacuum fields, thermal coupling, or quantum decoherence.

• No Empirical Evidence: All claims remain at the theoretical level. The absence of even a proof-of-concept MEMS prototype makes it impossible to assess feasibility We believe that despite the verifications to be made cited above, this described concept merit further study. If confirmation the fabrication of a prototype would be the last judge. This work on the energy balance of a M.E.M.S., which appears to be able to extract electrical energy from is a new, totally unexploited source of energy :. The theoretical results of this project seem sufficiently encouraging to justify the development of prototypes.

Future Perspectives : Several directions may be explored to advance this work toward experimental realization:

• Fabrication of a MEMS Prototype: Using established SOI processes, the core Casimir-piezoelectric structure could be fabricated and tested for spontaneous oscillation and charge generation under high vacuum conditions.

• Optimization of the Electrostatic Tuning Mechanism . Refining the design and control of the Coulombic counterforce could allow precise adjustment of the system's stability point, thereby enhancing energy output and frequency control

• Integration with Ultra-Low-Threshold CMOS Electronics . Coupling the system with high-impedance, low-power electronics would enable autonomous energy harvesting modules for use in nanoscale sensors or space applications.

• Extension to NEMS and 2D-Material Interfaces. Downscaling the architecture to NEMS and incorporating graphene or MoS_2 layers could dramatically enhance sensitivity to vacuum forces while reducing friction and energy losses.

• Experimental Quantification of Casimir-Induced Energy Transfer. Developing precision instrumentation to measure net energy extracted over time would help validate the theoretical model and quantify practical limits

This work opens a pathway for a new generation of self-powered microdevices operating at the edge of classical and quantum physics. While challenging, the experimental realization of such systems could lead to breakthroughs in autonomous electronics, quantum sensors, and fundamental vacuum physics.

As an inventor who has kept some important details confidential, I would like to collaborate in its development after signing a contract with the potential investor.

If its theoretical predictions are confirmed, it will trigger a scientific, technical and human revolution, because the

quantum vacuum can be used as a new source of energy both on Earth and in space with a considerable commercial market.

In the universe, everything is energy, everything is vibration, from the infinitely small to the infinitely large" Albert Einstein.
"A person who has never made mistakes has never tried to innovate." Albert Einstein

Reference

1. Reynaud, S., Lambrecht, A., Genet, C., & Jaekel, M. T. (2001). Fluctuations du vide quantique. Comptes Rendus de l'Academie des Sciences Series IV Physics, 9(2), 1287-1298.
2. Casimir, H. B. (1948). On the attraction between two perfectly conducting plates. In Proc. Kon. Ned. Akad. Wet. (Vol. 51, p. 793)
3. Casimir force between metallic mirrors | Springer Link. E.M. Lifshitz, Sov. Phys. JETP 2 73 (1956); E.M. Lifshitz and L.P. Pitaevskii, Landau and Lifshitz Course of Theoretical Physics: Statistical Physics Part 2 Ch VIII (Butterworth-Heinemann, 1980)
4. Sangouard, P. (1987). Modélisation de transistors polysilicium en couches minces sur isolants: conception et réalisation d'écrans plats à cristaux liquides et matrices actives (Doctoral dissertation, Paris 11).
5. (M. BARTHES, M. Colas des Francs SOLID MECHANICAL VIBRATIONAL PHYSICS, ESTP: (Special School of Public Works)
6. Sze, S. M. (2008). Semiconductor devices: physics and technology. John wiley & sons.
7. Deryagin, B. V., & Abrikosova, I. I. (1956). Direct measurement of the molecular attraction of solid bodies. J. Exp. Theo. Phys., 3, 819-829.
8. Techniques de l'Ingénieur 14/12/2012 : l'expertise technique et scientifique de référence « Applications des éléments piézoélectriques en électronique de puissance » Dejan VASIC : Maître de conférences à l'université de Cergy-Pontoise, Chercheur au laboratoire SATIE ENS Cachan, François COSTA : Professeur à l'université de Paris Est Créteil, Chercheur au laboratoire SATIE ENS Cachan
9. Wachel, J. C., & Bates, C. L. (1976). Techniques for Controlling Piping Vibration and Failures. ASME paper.
10. Parasuraman, J., Summanwar, A., Marty, F., Basset, P., Angelescu, D. E., & Bourouina, T. (2014). Deep reactive ion etching of sub-micrometer trenches with ultra high aspect ratio. Microelectronic engineering, 113, 35-39.
11. Marty, F., Rousseau, L., Saadany, B., Mercier, B., Français, O., Mita, Y., & Bourouina, T. (2005). Advanced etching of silicon based on deep reactive ion etching for silicon high aspect ratio microstructures and three-dimensional micro- and nanostructures. Microelectronics journal, 36(7), 673-677.